THE UNIVERSITY OF OKLAHOMA

GRADUATE COLLEGE

VIBRATIONAL SPECTRA OF LEAD ALKYLS

A THESIS

SUBMITTED TO THE GRADUATE FACULTY

in partial fulfillment of the requirements for the

degree of

DOCTOR OF PHILOSOPHY

BY

JASPER A. JACKSON, JR.

Norman, Oklahoma

1955

Downloaded from SHAREOK. Persistent Handle URL: https://hdl.handle.net/11244/149

VIBRATIONAL SPECTRA OF LEAD ALKYLS

APPROVED BY

J. Rud Nielsen

R. G. Fowler

Colin A. Plint

C. E. Spencer

Earl La Fon

THESIS COMMITTEE

ACKNOWLEDGMENTS

The author wishes to express his gratitude to Dr. J. Rud Nielsen, who directed the research, for his assistance and advice throughout the course of the work.

Thanks are also due to the following:

The Ethyl Corporation for the grant of a fellowship and gift of the samples;

Mr. George W. Thomson, of the Ethyl Corporation Research Laboratories, for his interest in the research;

Dr. E. E. Ferguson for his aid during the early stages of the investigation;

Mr. Louis Leistner, instrument maker for the physics department, who constructed the Raman irradiation apparatus;

Dr. N. A. Narasimham and Mr. James C. Albright for their advice and assistance in obtaining the infrared spectra;

Mr. Alva T. Stair, with whom the construction of the new low temperature Raman Irradiation apparatus was a joint undertaking, for his assistance in obtaining the low temperature Raman spectra;

Mrs. A. R. Autrey, who typed the thesis and drew some of the figures, for the care with which she executed this portion of the work.

TABLE OF CONTENTS

		Page
LIST OF TABLES		v
LIST OF ILLUSTRATIONS		vii
Chapter		
I.	INTRODUCTION	1
II.	STATEMENT OF THE PROBLEM	4
III.	EXPERIMENTAL	5
	Raman Spectra	5
	Infrared Spectra	28
	Purity of Samples	28
IV.	EXPERIMENTAL RESULTS	30
V.	POSSIBLE MOLECULAR SYMMETRIES	68
	Introduction	68
	Possible Symmetry of TML	68
	Possible Symmetry of TMEL	71
	Possible Symmetry of DMDEL	71
	Possible Symmetry of MTEL	77
	Possible Symmetry of TEL	80
VI.	INTERPRETATION OF VIBRATIONAL SPECTRA OF TML	86
VII.	INTERPRETATION OF THE SPECTRA OF TMEL, DMDEL, MTEL, AND TEL	101
VIII.	COMPARISON OF THE SPECTRA OF TEL AND TEL-d_{20}	118
IX.	SUMMARY AND CONCLUDING REMARKS	123
BIBLIOGRAPHY		128

LIST OF TABLES

Table		Page
I.	Exposure Times and Temperatures for the Strongest Raman Spectra Obtained.	27
II.	Raman Spectrum of Tetramethyllead (TML)	42
III.	Raman Spectrum of Crystalline TML	44
IV.	Raman Spectrum of Trimethylethyllead (TMEL) . .	45
V.	Raman Spectrum of Dimethyldiethyllead (DMDEL) .	48
VI.	Raman Spectrum of Methyltriethyllead (MTEL) . .	50
VII.	Raman Spectrum of Tetraethyllead (TEL).	54
VIII.	Raman Spectrum of $Pb(C_2D_5)_4$ (TEL-d_{20})	58
IX.	Raman Spectrum of Triethylbismuth	61
X.	Infrared Spectrum of Methyltriethyllead (MTEL).	62
XI.	Infrared Spectrum of Tetraethyllead (TEL) . . .	64
XII.	Infrared Spectrum of $Pb(C_2D_5)_4$ (TEL-d_{20}). . . .	65
XIII.	Classification of Normal Vibrations of TMEL . .	73
XIV.	Classification of Normal Vibrations of DMDEL. .	76
XV.	Classification of Normal Vibrations of MTEL . .	79
XVI.	Classification of Normal Vibrations of TEL. . .	85
XVII.	Distribution of Fundamental Vibrations for TML.	87
XVIII.	Number of Raman Active Fundamentals	102
XIX.	Number of Infrared Active Fundamentals.	104

LIST OF ILLUSTRATIONS

PLATE		Page
I.	Possible Configurations of Lead-Carbon Skeleton of TMEL.	72
II.	Possible Configurations of Lead-Carbon Skeleton of DMDEL	75
III.	Possible Configurations of Lead-Carbon Skeleton of MTEL.	78
IV.	Possible Configurations of Lead-Carbon Skeleton of TEL	82
Figure		
1.	Raman Irradiation Apparatus	8
2.	Irradiation Apparatus (Vertical Cross-Section).	10
3.	Mounting of Raman Tube for Low Temperature Work	10
4.	Dewar Flask for Low Temperature Raman Irradiation Apparatus.	18
5.	Dewar Flask and Associated Parts-Assembled. . .	19
6.	Mercury Lamp for Low Temperature Raman Irradiation Apparatus.	20
7.	New Low Temperature Raman Irradiation Apparatus	21
8.	Short Raman Exposures	34
9.	Longest Raman Exposures	35
10.	Infrared Spectrum of MTEL 3 to 15 Micron Region.	36
11.	Infrared Spectrum of MTEL 15 to 25 Micron Region	37

12. Infrared Spectrum of TEL 3 to 15 Micron Region. 38

13. Infrared Spectrum of TEL 15 to 25 Micron Region 39

14. Infrared Spectrum of TEL-d_{20} 3 to 15 Micron Region. 40

15. Infrared Spectrum of TEL-d_{20} 15 to 25 Micron Region 41

16. Tetramethyllead in Eclipsed Configuration . . . 69

17. Orientation of Methyl Groups in Eclipsed and Staggered Configurations. 69

18. Resolution of Raman Bands in TML. 91

19. Normal Vibrations of XY_4 Molecule 93

20. Observed Raman Spectra of $(CH_3)_4$ X-Type Molecules 95

21. Observed Spectra of Lead Alkyls 107

22. Observed Spectra of Silicon Alkyls. 108

23. Observed Spectra of TEL and TEL-d_{20} 119

VIBRATIONAL SPECTRA OF LEAD ALKYLS

CHAPTER I

INTRODUCTION*

Although a number of workers have studied the vibrational spectra of lead alkyls, the spectral data for most of the compounds have been incomplete, since the lead alkyls are toxic and chemically unstable, some of them being extremely photosensitive. The first Raman data for TML and TEL were reported by Duncan and Murray (5) in 1934. Raman data for TEL were also published by N. G. Pai (15) in 1935. Photodecomposition of the lead alkyls constituted a serious difficulty for these workers. Lippincott and Tobin (14) have reported more complete Raman data for TML, and Hall (7) has recently obtained Raman spectra for the series TML, TMEL, DMDEL, MTEL, and TEL, including weak polarization exposures for TML, MTEL, and TEL. However, he also experienced considerable difficulty with photodecomposition.

The first infrared data for TML and TEL were reported

---

*In this work the following abbreviations will be used: TML - tetramethyllead, TMEL - trimethylethyllead, DMDEL - dimethyldiethyllead, MTEL - methyltriethyllead, TEL - tetraethyllead, TEL-d_{20} - deuterated tetraethyllead $Pb(C_2D_5)_4$.

in 1933 by Kettering and Sleator (11). In 1946, Swanson (18) obtained spectra of both of these compounds in addition to the spectrum of TML in the vapor phase. In 1950 Pitzer and Sheline (17) reported infrared data for TML in liquid and vapor phases in the wavelength range from 2 to 25 microns. The data of the other workers were restricted to the 2 to 15 microns range.

Infrared spectra, in the range 2 - 15 microns, for the compounds TML, TMEL, DMDEL, MTEL, and TEL have been obtained at the Ethyl Corporation Research Laboratories (6). The instrument used in this work was a Beckman IR-2 infrared spectrometer, an instrument of moderate resolution.

In 1947, Young, Koehler, and McKinney (19) made an assignment of the fundamental vibrational frequencies of TML, based on the rather incomplete data available at that time. Pitzer and Sheline (17), in 1950, Lippincott and Tobin (14), in 1951, and Hall (7), in 1952, using newer data, have extended and modified the basic assignment of Young, et al.

It is desirable to have good Raman and infrared data before attempting to determine the normal vibration frequencies. This is especially true for complex molecules such as the lead alkyls.

The infrared spectra of all the lead alkyls in the series mentioned have been obtained, but, for most, only on instruments of moderate resolution, and only for TML in the range 15 to 25 microns. The difficulty with photodecomposi-

tion in the unstable lead alkyls, experienced by the various workers, resulted in a scarcity of good Raman data for all these compounds, with the exception of TML. However, the possibility existed that by cooling the samples, the rate of photodecomposition could be reduced sufficiently to permit good Raman spectra to be obtained. Therefore, it was decided to attack anew the problem of obtaining spectra, particularly Raman spectra, of the lead alkyls.

CHAPTER II

STATEMENT OF THE PROBLEM

The objectives of this investigation have been:

(1) To design apparatus and develop experimental methods for obtaining Raman spectra at low temperatures.

(2) To obtain as complete Raman and infrared spectra as possible for the series of lead alkyls TML, TMEL, DMDEL, MTEL, TEL, and TEL-d_{20}, and Raman spectrum of triethylbismuth.

(3) To give as complete an interpretation as possible of the spectra of these compounds.

CHAPTER III

EXPERIMENTAL

Raman Spectra

Raman Spectrograph

The three-prism spectrograph used in obtaining the Raman spectra has been described by Claassen (2) and Hudson (10). The small shield provided by Claassen for shielding the film from the direct Rayleigh-scattered light of the 4358 A^{o} line of mercury was not used, since the Raman scattered light from the lead alkyls was quite strong, and since a search was made for very small Raman shifts.

Photographic Emulsion and Developer

Eastman Kodak Tri-X Pan sheet film was used in the photographic recording of all the Raman spectra except that of deuterated TEL, for which Eastman Kodak Royal Pan sheet film was used. Both films were developed 12 minutes at 18° - 20°C in DK-60a.

Kodak Royal Pan is a new photographic product that is just as sensitive as Tri-X Pan sheet film in the region of 4358 A^{o} and is much more sensitive than Tri-X Pan near

5400 A°. Royal Pan also has much greater "latitude" than Tri-X Pan, i.e., it can be developed to a much greater extent before showing fog due to development of unexposed grains. One test film was developed 20 minutes at 20°C in DK-60a without showing appreciable background. In addition, Royal Pan seems to have finer grain than Tri-X Pan.

Measurement of Raman Shifts

An iron spectrum was photographed beside each Raman spectrum. The film was enlarged 22.5 times directly and printed on photographic paper. These prints were then used to measure the frequencies of the Raman bands by linear interpolation as described by Claassen and Hudson.

Raman Irradiation Apparatus

Irradiation efficiency tests. The first apparatus was an experimental pilot model constructed to determine the feasibility of using hairpin-shaped lamps arranged as shown in vertical cross section in Figs. 2a and 2b, page 10. The hairpin-shaped mercury lamps were made in the glass blowing laboratory of the Phillips Petroleum Company. A series of tests were made to determine the optimum spacing of the lamp, filter-lens, reflector and Raman tube. In these tests a holder was built which would permit the spacing of these components to be changed. A Raman tube was filled with water to which a slight trace of milk had been added. This gave it a slightly turbid appearance due to the Tyndall scattering of

the light by the milk. The intensity of this scattered light, which is proportional to the intensity of the light incident on the Raman tube, was measured by placing a photoelectric cell at the window of the Raman tube and reading the current from the cell on a microammeter. In this way the effective irradiation could be observed as the spacing of the components of the irradiation apparatus were varied.

The conclusion reached in these tests was that for maximum irradiation of the Raman tube, the components should be placed as closely together as possible. However, the cooling requirements for the lamp place a lower limit on the spacing. When this had been determined, the apparatus shown in Fig. 1, page 8, for obtaining the Raman spectra of liquids both at room temperature and at low temperature was designed and constructed.

Description of apparatus. The mercury lamp was of the low pressure "Toronto" type in which the electrodes are internally water cooled. The barrel was bent in the shape of a hairpin with both electrodes housed at the rear of the apparatus. Lamp, filter-lens, and Raman tube were all held in a horizontal position with the axis of the Raman tube coincident with the optical axis of the spectrograph collimator. The axis of the Raman tube, the filter-lens and the lamp barrels were arranged so as to lie in a plane inclined at 45° to the horizontal. This was done to facilitate the obtaining of depolarization ratios by the single exposure

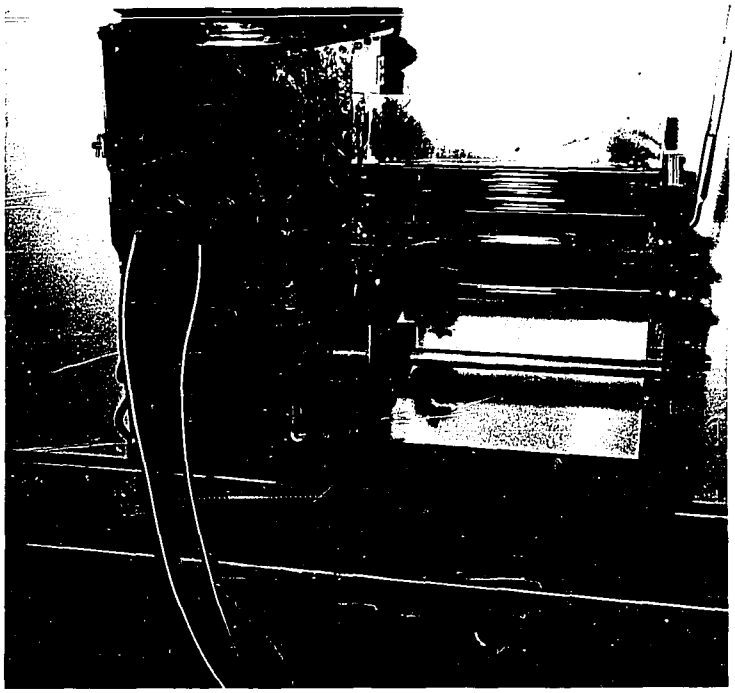

Figure 1.

Raman Irradiation Apparatus

method.

The reflecting surfaces nearest the mercury lamp were hinged to allow the reflectors to be swung away from the filter-lens as shown in Fig. 2a, page 10. This facilitated inspection and cleaning of the lamp barrel and the reflecting surfaces. The hinged surfaces were of polished sheet aluminum. The remaining reflecting surfaces surrounding the Raman tube were of aluminum foil.

The Raman tube was supported at front and rear by two washers of phenolic resin. The washers were held by brass collars screwed into aluminum mounts at the front and rear of the apparatus. The rear mount could be moved forward or backward on aluminum rods on either side of the apparatus. This permitted use of Raman tubes of various lengths up to a maximum length of 25 cm. The use of aluminum foil as the reflecting surface around the Raman tube permitted rapid changing of reflectors for Raman tubes of different length.

The filter-lens was a Pyrex tube with outside diameter of 5.1 cm and inside diameter of 4.7 cm. Its purpose was twofold. When filled with liquid (e.g. water), it acted as a cylindrical condensing lens to help focus the light from the mercury lamp on the Raman tube. When filled with a liquid capable of absorbing certain wavelengths of the mercury light, it acts as a filter to shield the sample in the Raman tube from undesired radiations. In the present work, a one-fourth saturated solution of $NaNO_2$ in water was used

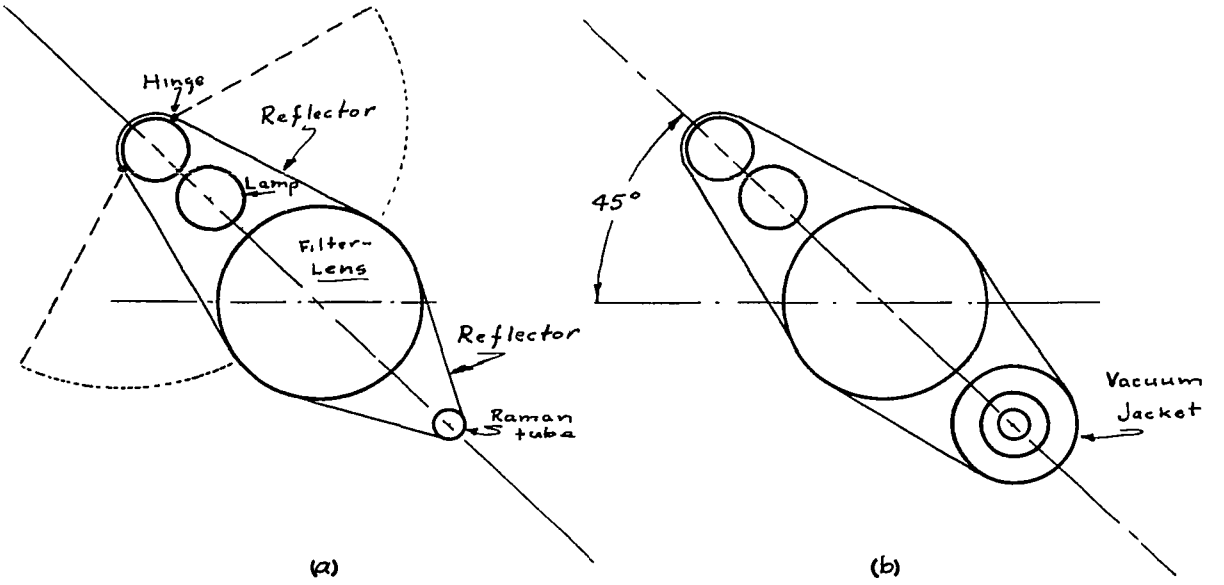

ROOM TEMPERATURE ARRANGEMENT

LOW TEMPERATURE ARRANGEMENT

IRRADIATION APPARATUS
(VERTICAL CROSS SECTION)

FIG. 2

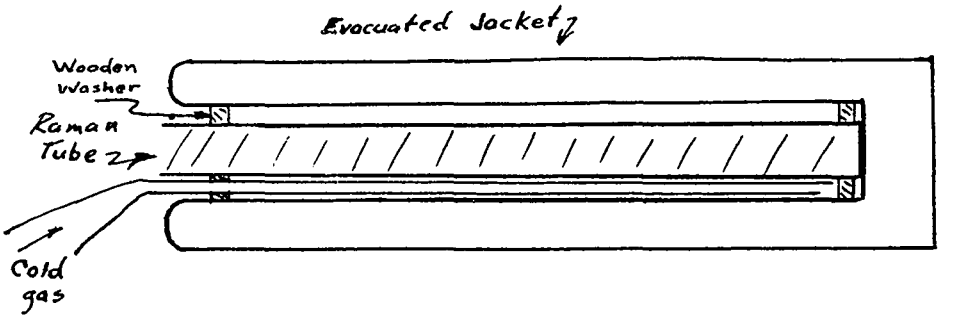

MOUNTING OF RAMAN TUBE FOR LOW TEMPERATURE WORK

FIG. 3

to absorb practically all mercury light with wavelengths shorter than about 4300 A^{o}.

Two walls of the lamp housing were hinged to permit easy access to the electrodes. Connections for the cooling water, the direct current, and the high-voltage, high frequency starting current were made through the side of the lamp housing, as shown in Fig. 1, page 8.

The lamp was cooled by drawing air over it by means of a powerful squirrel-cage blower, connected to an eight-inch pipe on top of the lamp housing, as shown in Fig. 1, page 8. Air was drawn from the room through an opening at the front end of the housing, along the length of the lamp barrels into the box containing the electrodes and then up into the blower. Additional small holes were drilled through the reflector along the lamp barrel to prevent the rear of the barrel from overheating. Holes were also drilled in the bottom of the box containing the electrodes to provide additional air cooling for the electrodes. To prevent stray, unfiltered mercury light from getting on the sample, a light trap was placed over the air intake opening at the front end of the lamp housing.

In the present work, the lamp was operated at a current of 10 amperes with appropriate series resistance. This was about the maximum possible current which could be used without overheating the lamp.

Preliminary Raman Exposures

Usually, the 4358 A° line of mercury is used as the incident, or "exciting," radiation. However, several other possible exciting mercury lines fall within the range of the spectrograph used, in particular, those at 4047 A° and 5461 A°. The dispersion of the spectrograph is 15 A°/mm at 4358 A°, 34 A°/mm at 5000 A°, and about 7 A°/mm at 4047 A°.

At the start of the present work, there were on hand two samples each of TMEL and DMDEL. These decompose at room temperature when irradiated with light of wavelength 4358 A°. It was attempted, therefore, to use the 5461 A° (green) line of mercury as the exciting line. It was isolated with a neodymium amonium nitrate filter as described by Collins (3). Although the samples showed very little decomposition after long exposure to this radiation, a combination of unfavorable factors made further pursuit of this line of investigation unprofitable. The most serious drawbacks were the reduced resolution of the spectrograph in the 5400 A° region, and the decrease in the intensity of the scattered light which varies inversely as the fourth power of the wavelength of the scattered radiation.

Low Temperature Technique

Cold air cooling system. In order to reduce the photochemical decomposition of the samples, it was necessary to expose them at low temperature. The apparatus used for

this purpose consisted of a transparent, double-walled, evacuated Pyrex jacket (3 cm outside diameter, 1.7 cm inside diameter, 27 cm in length) in which the Raman tube was held by wooden washers, as shown in Fig. 3, page 10. The jacket was mounted in the apparatus shown in Fig. 1, page 8. On the first experiments, the sample was cooled by a stream of cold air introduced into the jacket by a long glass tube (3 mm outside diameter, 1 mm inside diameter) that ran parallel to the Raman tube inside the jacket. The glass tube carried the cold air to the closed end of the jacket from which point it flowed around the Raman tube toward the open end.

The air was obtained from the house compressed air supply and was partially dried by flowing through several tubes containing a drying agent. It was then precooled and dried further by flowing successively through two glass U-tubes (2 cm outside diameter, 25 cm deep) immersed in Dewar flasks containing a mixture of dry ice and acetone. The remaining water vapor was frozen out in these two tubes. The dry, precooled air then flowed through a copper coil immersed in another Dewar flask filled with dry ice and acetone.

A flow meter was placed in the air line, and the rate of flow of air was calibrated against the temperature as read on a pentane thermometer placed in the jacket in place of the Raman tube. By adjusting the rate of flow of air, temperatures as low as -50°C could be obtained at the closed end of the jacket. An increase in temperature of about 20°C was

observed along the jacket from the closed to the open end.

A very great increase in the rate of flow of air was required to lower the temperature from -40°C to -50°C. Therefore, spectra at temperatures below -40°C were not attempted with this arrangement.

Cold nitrogen cooling system. In order to obtain lower temperatures, cold oil-pumped dry nitrogen was used to cool the sample. The nitrogen gas was cooled by allowing it to flow from standard 224 cu. ft. tanks at approximately 2200 psi pressure through a copper coil immersed in a Dewar flask filled with liquid nitrogen.

To check the temperature more accurately, a copper-constantin thermocouple was inserted in the vacuum jacket with the cold junction at the closed end of the jacket, the warm junction of the thermocouple being inserted in a mixture of ice and water. The thermoelectric current was read on a sensitive microammeter and was calibrated against the pentane thermometer. A temperature increase of about 20°C was again observed along the length of the jacket between its closed and open ends.

Since the walls of the vacuum jacket are unsilvered, the outside of the jacket is cooled by radiation. When the atmospheric humidity was high, difficulty with condensation of atmospheric moisture was sometimes encountered. This was relieved by allowing air from the house compressed air supply to flow over the outer surface of the jacket. A separate

stream of air was allowed to flow over the outer window of the jacket, since any moisture which condensed here would prevent light from the Raman tube from reaching the spectrograph.

It was decided not to use a lens system between the Raman tube and the spectrograph, but rather to place the window of the Raman tube as close to the slit as possible. For this purpose, the yoke, which was mounted over the slit of the spectrograph and which held a prism ordinarily used for deflecting light from an iron arc onto the slit of the spectrograph, was removed. The front window of the vacuum jacket was placed about 2 cm from the slit of the spectrograph. This allowed sufficient space between the vacuum jacket and the slit for the flow of air across the window of the jacket and also sufficient space to insert a white card at 45° to the axis of the spectrograph to reflect light from the iron arc onto the slit of the spectrograph. The space between the outer and inner windows of the vacuum jacket was about 1 cm. The window of the Raman tube was placed in contact with the inner window of the vacuum jacket. Thus, the window of the Raman tube was about 3 cm from the slit of the spectrograph.

The use of the low temperature apparatus made it convenient to distill the sample into the Raman tube after the tube had been placed in the irradiation apparatus. When cold nitrogen was allowed to flow over the Raman tube, as described above, the liquid in the darkened ampule, kept at room

temperature, would distill into the Raman tube in about one hour.

Several exposures with this apparatus were accidentally terminated, as follows: The nitrogen gas expands and cools upon emerging from the high pressure tank into the pressure regulator on the tank. If the rate of flow is increased sufficiently, the gas, precooled by expansion, will condense in the copper coil immersed in liquid nitrogen, and liquid nitrogen will issue from the glass tube inside the vacuum jacket. The windows of the Raman tube are sealed lightly onto the end of the Raman tube to prevent distortion of the plane window surface. When the liquid nitrogen suddenly comes in contact with the Raman tube, strains are set up and the seal may crack, with resultant loss of the sample. This occurred occasionally, even when the Raman tube had been well annealed in an oven before use. In some of these accidents, a little of the sample leaked out of the Raman tube, contaminating the laboratory for several days.

The original Dewar flask used to hold the copper coil and liquid nitrogen was of one liter capacity. This required the operator to be in constant attendance. Dewar flasks of five liter capacity were therefore substituted. When one of these was used, the apparatus required attention only about every hour. It had been hoped that the apparatus could be made to require even less attention by running the dry nitrogen gas successively through two copper coils, each coil

being immersed in liquid nitrogen in a separate five liter Dewar flask. Unfortunately, the heat capacity of the resulting system was so large that the temperature was difficult to control, and much difficulty was encountered in the condensation of nitrogen gas within the copper coils due to excessive flow of nitrogen gas. This resulted in the loss of two samples from accidents of the type described above. Therefore, this method was abandoned and one five-liter Dewar was used.

New Low-Temperature Apparatus

The apparatus used for the low temperature Raman work, described above, still required the attention of the operator at least once an hour. It was desirable to have an apparatus which could be left unattended for longer periods of time. It was also desirable to eliminate the use of nitrogen gas in the cooling system, since the cooling of the warm gas consumed large amounts of liquid nitrogen. Other undesirable features of the old apparatus were the temperature gradient along the Raman tube and the difficulty of controlling the temperature closely by adjusting the rate of flow of the nitrogen gas.

For these reasons, a new apparatus for obtaining Raman spectra at low temperature was designed. This apparatus is shown in Figs. 4, 5, 6, and 7, pages 18 through 21. It consists of a large Dewar flask that is silvered at the

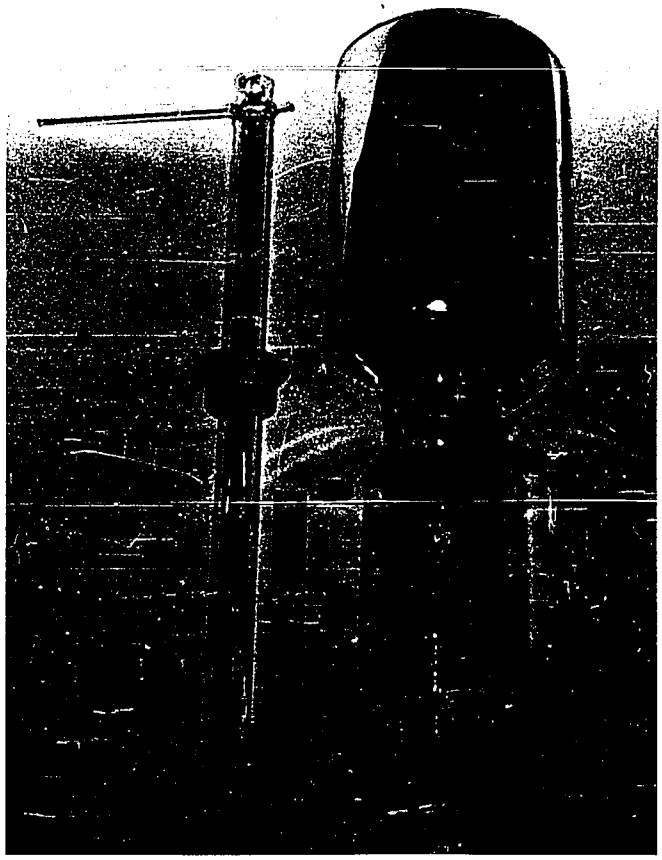

Figure 4.

Dewar Flask for Low Temperature
Raman Irradiation Apparatus

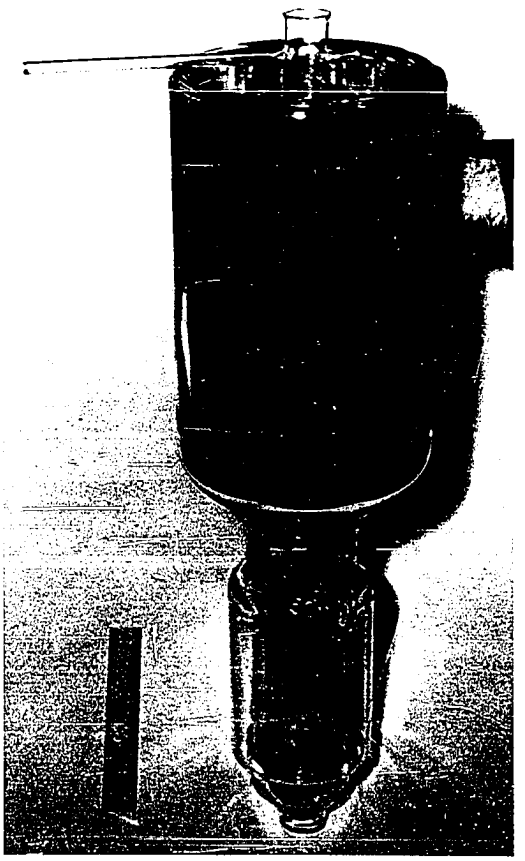

Figure 5.

Dewar Flask and
Associated Parts - Assembled

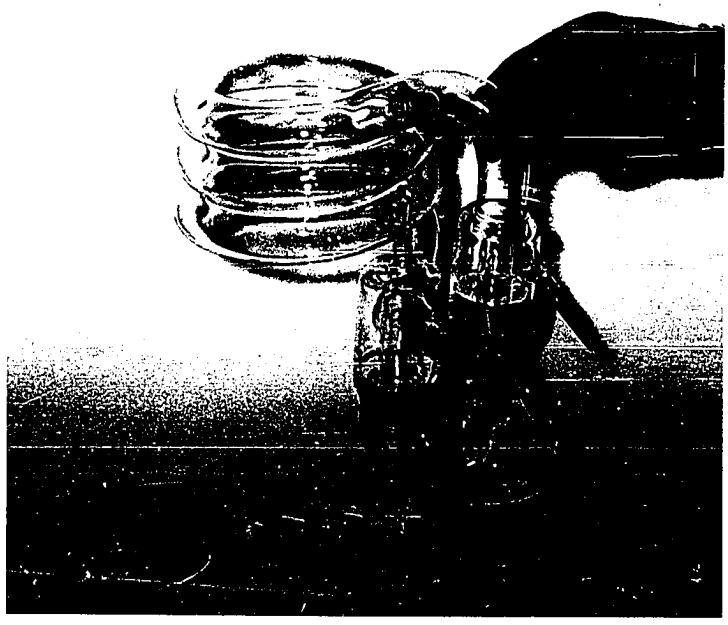

Figure 6.

Mercury Lamp for Low Temperature
Raman Irradiation Apparatus



Figure 7.

New Low Temperature
Raman Irradiation Apparatus

top but has a transparent section at the bottom, through which the sample is irradiated by a mercury lamp. The barrel of this lamp is shaped in the form of a helix surrounding the transparent section of the Dewar. An integral part of the Dewar is a jacket around the transparent section through which a filter solution may be circulated.

The transparent section of the Dewar flask has two plane windows on the bottom through which the light scattered by the sample is taken to the spectrograph by means of a prism and lens system.

Within the Dewar flask is a Pyrex tube with a plane window on the bottom. This tube is centered in the Dewar by Lucite washers and extends the full length of the Dewar flask. The Raman tube is centered inside this Pyrex tube, also with Lucite washers. The upper end of the Pyrex tube is sealed and provisions are made for evacuating the tube and introducing a dry gas such as N_2 or He. The purpose of using a dry gas is to prevent the condensation of atmospheric moisture. In addition, the thermal conduction between the liquid nitrogen and the Raman tube can be controlled by varying the pressure of the gas. A heating coil is also wound around the Raman tube to give additional temperature control.

The inside of the lamp housing is coated with a diffuse reflecting coating of magnesium oxide. The lamp is cooled by drawing air across it with the large squirrel cage blower, mentioned above.

This apparatus, however, was not completed in time

to permit its use with the lead alkyls, and all spectra were obtained with the apparatus in Fig. 1, page 8.

Temperature Dependance of Photodecomposition

It was found that the condition of the sample could best be determined by looking into the end of the Raman tube. A very small amount of colloidal decomposition product (presumably colloidal lead) was sufficient to make the sample appear turbid when viewed through the Raman window. This condition is reached long before the decomposition can be detected by looking laterally at the Raman tube.

It was found that if TEL is exposed to room light, at room temperature, it begins to appear turbid, when viewed through the window of the Raman tube, in about fifteen seconds. Therefore, the samples of all compounds except TML were handled only under a dim, amber-colored light until their temperature had been sufficiently reduced.

A temperature of $-40^{\circ}C$ was sufficiently low to prevent noticeable decomposition in TMEL when exposed to the 4358 A° line of mercury. Several spectra of this compound were taken at this temperature, the longest exposure time being thirty hours.

A temperature of $-40^{\circ}C$, however, was not sufficiently low to prevent or substantially reduce the decomposition of DMDEL exposed to 4358 A°. In fact, the sample became turbid after about twenty minutes' exposure.

This temperature was entirely inadequate for the study of TEL. A two hour exposure of TEL was made at -70°C afterwhich the sample was completely opaque when viewed through the window of the Raman tube, indicating that it had become turbid after a much shorter exposure at this temperature.

A method was devised of examining the sample through the window of the Raman tube by means of a mirror while the exposure was in progress. It was found that at -100°C TEL would begin to appear turbid after about six hours, whereas an exposure of forty-eight hours was made of TML at room temperature with no sign of decomposition.

According to the Handbook of Chemistry and Physics, TEL freezes at -136°C at a pressure of one atmosphere. It was therefore decided to expose it at -125°C. When this temperature is maintained, one tank of nitrogen gas lasts about eight to ten hours, and liquid nitrogen is consumed at approximately 1.25 to 1.50 liters per hour.

At -125°C TEL showed no detectable sign of decomposition after eighteen hours' exposure to 4358 A° mercury radiation.

Only a very weak Raman spectrum of triethylbismuth was obtained, since this compound decomposed after a few minutes' exposure to 4358 A° radiation at -125°C.

Replacement of Mercury Lamp

The light from a mercury arc is rich in ultraviolet

radiation, and, eventually, the Pyrex barrels of a mercury lamp will darken under the action of this short wavelength radiation. The barrels of the lamp had become quite brown, and it appeared possible that most of the 4358 A^{o} radiation was being absorbed by the glass. Claassen (2) states that the brown coloration can be removed by baking the lamp in an oven while evacuating it. However, the brown coloration thus removed returns fairly soon after the lamp is returned to use.

Potassium hydroxide is used as an electrolyte in cleaning the tungsten electrodes of the mercury lamp. It was found during the course of such cleaning that KOH would remove the brown coloration from the barrel of the lamp. Pyrex is slightly soluble in KOH at room temperature (solubility as a function of temperature is given by Corning [4]). It is presumed that the KOH dissolves a thin layer of Pyrex on the inner surface of the barrel. This layer would be the most discolored since layers further from the inner surface would be shielded from some of the ultraviolet radiation by the discoloration of the innermost layers. It is believed that a lamp so cleaned will not become discolored quickly upon return to service, as is said to be the case with lamps cleaned by the baking process. A lamp cleaned with KOH was used for some time in this laboratory with satisfactory service. However, no direct comparison of the two methods could be made since no lamp cleaned by the baking process was

available.

However, since the exposure time is limited by the supply of gaseous and liquid nitrogen, it was decided to replace the lamp with darkened barrels in the low-temperature apparatus with a new lamp. A comparison of exposures of TEL with the old and new lamps indicated that the irradiation had been increased by a factor of 10.

Final Exposures on Liquid Samples

Exposures were made on all compounds with the new lamp. The spectra obtained are far more complete than any previous spectra of the lead alkyls.

The longest exposure times and the temperatures at which they were made are given in Table I, page 27.

No exposures of TML had been made except at room temperature. It was considered desirable to take an exposure at lower temperature for comparison purposes. However, when the temperature was lowered past $0^{\circ}C$, the sample became turbid, indicating that it contained a slight amount of water. The turbidity precluded any work with TML in the liquid state at low temperature.

Spectra of Crystalline TML

It was possible to freeze TML and obtain a spectrum of it in the crystalline state. When the temperature was lowered to $-70^{\circ}C$, the sample froze into a polycrystalline mass, starting at the Raman window and progressing rapidly

TABLE I

EXPOSURE TIMES AND TEMPERATURES FOR THE STRONGEST RAMAN SPECTRA OBTAINED

Compound	State	Max Exposure Time	Temperature
TML	Liquid	48 hours	25°C
TML	Liquid	38 hours	10°C
TMEL	Liquid	16 hours	- 70°C
DMDEL	Liquid	4½ hours*	-120°C
MTEL	Liquid	13 hours	-100°C
TEL	Liquid	18 hours	-120°C
$TEL\text{-}d_{20}$	Liquid	26 hours	-120°C
TML	Crystalline	1 hour	- 70°C
Triethylbismuth	Liquid	10 min	-125°C

*Accidentally terminated.

toward the rear of the Raman tube. Since some of the Raman bands in TML are very strong, it was possible to get a fair spectrum of it in the crystalline state in spite of the intense scattering of mercury light on account of its "snowy" appearance in this state.

An attempt was also made to get spectra of TMEL, MTEL, and TEL in the crystalline state. TMEL and MTEL were solidified, but it is believed that they formed glasses, or supercooled liquids, since their spectra were almost identical with those in the liquid state. It was not possible to solidify TEL, even at -195°C.

Infrared Spectra

Infrared spectra were obtained for TML, TMEL, TEL, and TEL-d_{20} in the liquid state in the region from 3 to 25 microns using a Perkin-Elmer model 112 infrared spectrometer. An attempt was made to obtain the spectrum of TEL vapor. However, the vapor pressure was so low that, even with a path length in excess of one meter, only a very weak spectrum was obtained.

Purity of Samples

The samples used in this investigation were kindly supplied by the Ethyl Corporation.

The per cent of lead alkyl in the samples in all instances was greater than 99 per cent. The samples of TML and TEL were nearly 100 per cent pure. In the case of TMEL,

DMDEL, and MTEL, the purity was equal to, or greater than, 96 per cent. For these intermediate compounds, the principal impurities were the neighboring lead alkyls. In all samples, there may have been traces of ethane, ethylene, butane, and methylethylchloride. The products of photodecomposition are probably butane, ethane, ethylene, plus metallic lead.

The sample of TEL-d_{20} was believed to have been completely deuterated. It probably contained less than 1 per cent impurity, which was believed to have been completely deuterated hydrocarbon.

CHAPTER IV

EXPERIMENTAL RESULTS

Reproductions of the Raman spectra of the different lead alkyls and of triethylbismuth obtained with short exposure times are shown in Fig. 8, page 34. The spectra obtained with the longest exposures are shown in Fig. 9, page 35. The observed Raman shifts for the different compounds are given in Tables II to IX, pages 42 through 61. The first column gives the wave number in cm^{-1}. In the second column is given an indication, first, of the relative intensity, then of the appearance, and, finally, qualitative information on the depolarization ratio for the band, if such is available. The abbreviations used are s strong, m medium, w weak, v very, sh sharp, d diffuse, b broad, p polarized, dp depolarized. The term "diffuse" is applied to those bands that show a gradual reduction in intensity to both sides from the center of the band, while the term "broad" is used if the band has a central "plateau" with a fairly sharp decrease in intensity on either side.

The observed infrared spectra of TEL, TEL-d_{20}, and MTEL are reproduced in Figs. 10 to 15, pages 36 through 41.

The absorption maxima are listed in Tables X to XII, pages 62 through 67, together with their description and interpretation.

The observed spectrum of TML is not reproduced, since it is almost identical with that obtained by Swanson (18).

In the Raman spectrum of TML several new bands were found at 342 and 692 cm^{-1} and in the region 1800 to 2600 cm^{-1}. The bands reported by Hall at 1235, 1340, and 1506 cm^{-1} were not observed, and are believed to have been excited by mercury lines near 4000 A^{o} which were absorbed by the $NaNO_2$ filter in the present work.

No previous infrared and Raman spectra of TEL-d_{20} have been obtained. The Raman spectra of TMEL, DMDEL, MTEL, and TEL presented are much more complete than any previous spectra. The principal new infrared data result from the study of MTEL and TEL in the CsBr region. The spectra for this region show that the fundamentals at about 445 and 465 cm^{-1} are infrared active in both MTEL and TEL. In addition, the infrared bands at about 662 and 727 cm^{-1} were resolved. The infrared spectra for MTEL and TEL also showed that the fundamental at about 1155 cm^{-1} is infrared active, but, apparently, that at 1164 cm^{-1} is not.

One of the most noticeable features of the Raman spectra of the lead alkyls is the great difference in intensity among different bands. Another striking feature is the similarity of the spectra of the compounds containing ethyl

groups, and the contrast between these and the spectrum of TML.

There are several frequencies that are practically unchanged throughout the whole series, TML to TEL. These are at approximately 130, 462, 475, 1157, and 1169 cm^{-1}. The addition of one ethyl group in going from TML to TMEL produced changes in the Raman spectra that remain throughout the series. In the 2800 to 3000 cm^{-1} region, several new bands make their appearance. The most striking difference between the spectra of TML and TMEL is found in the region 1300 to 1500 cm^{-1}. In place of the two diffuse bands found in the Raman spectrum of TML, TMEL has three sharp bands, one of which may be double, and possibly a faint, very diffuse band. The three sharp bands also occur practically unchanged in the spectra of DMDEL, MTEL, and TEL. The two strong bands at 1157 and 1169 cm^{-1} in TML appear nearly unchanged in frequency throughout the series, both bands being slightly more diffuse than in TML. The strong, sharp Raman band at approximately 1015 cm^{-1} and the weak, sharp band at approximately 960 cm^{-1} are characteristic of all the lead alkyls containing ethyl groups. Sufficiently strong exposures were obtained for TMEL, MTEL, and TEL to show characteristic bands near 936 and 916 cm^{-1}.

A noticeable feature of the spectra is the disappearance of the diffuse band found at about 769 cm^{-1} in TML. A weaker band appears at this frequency in TMEL but not in the spectra of MTEL and TEL. A band appears at 728 cm^{-1} in the

spectrum of MTEL, but not in the spectrum of TEL. There is a very weak, diffuse band near this frequency in TMEL. MTEL and TEL show a set of Raman bands at approximately 640, 660, and 675 cm^{-1} that do not appear in the spectra of the other molecules.

The strong Raman bands at 462 and 475 cm^{-1} in TML appear practically unchanged throughout the entire series, the band at approximately 475 cm^{-1} being slightly broader than in TML. TMEL has a band at about 235 cm^{-1} which does not appear in TML. The remaining members of the series each show two broad bands near this frequency, their separation increasing from DMDEL to TEL. The strong, diffuse band near 132 cm^{-1} in TML is shifted slightly toward lower frequencies in the other members of the series. In TML, this band has an asymmetric appearance with a shoulder extending toward higher frequencies. In TMEL, it is nearly symmetrical; in DMDEL it is asymmetric with a shoulder extending toward lower frequencies. In MTEL and TEL this band has a broader and perhaps slightly asymmetric appearance with a shoulder toward lower frequencies. However, scattering from the 4358 A^{o} mercury line makes this observation somewhat uncertain. The spectrum of TMEL shows, in addition, three very sharp bands at 127, 134, and 144 cm^{-1} superposed on the diffuse band with center at 135 cm^{-1}. The spectrum of MTEL shows a very sharp band at 60 cm^{-1} which may be spurious. However, a close check of other spectra which showed spurious lines near the 4358 A^{o} showed no bands near 60 cm^{-1}, so that the interpretation of this band is in doubt.

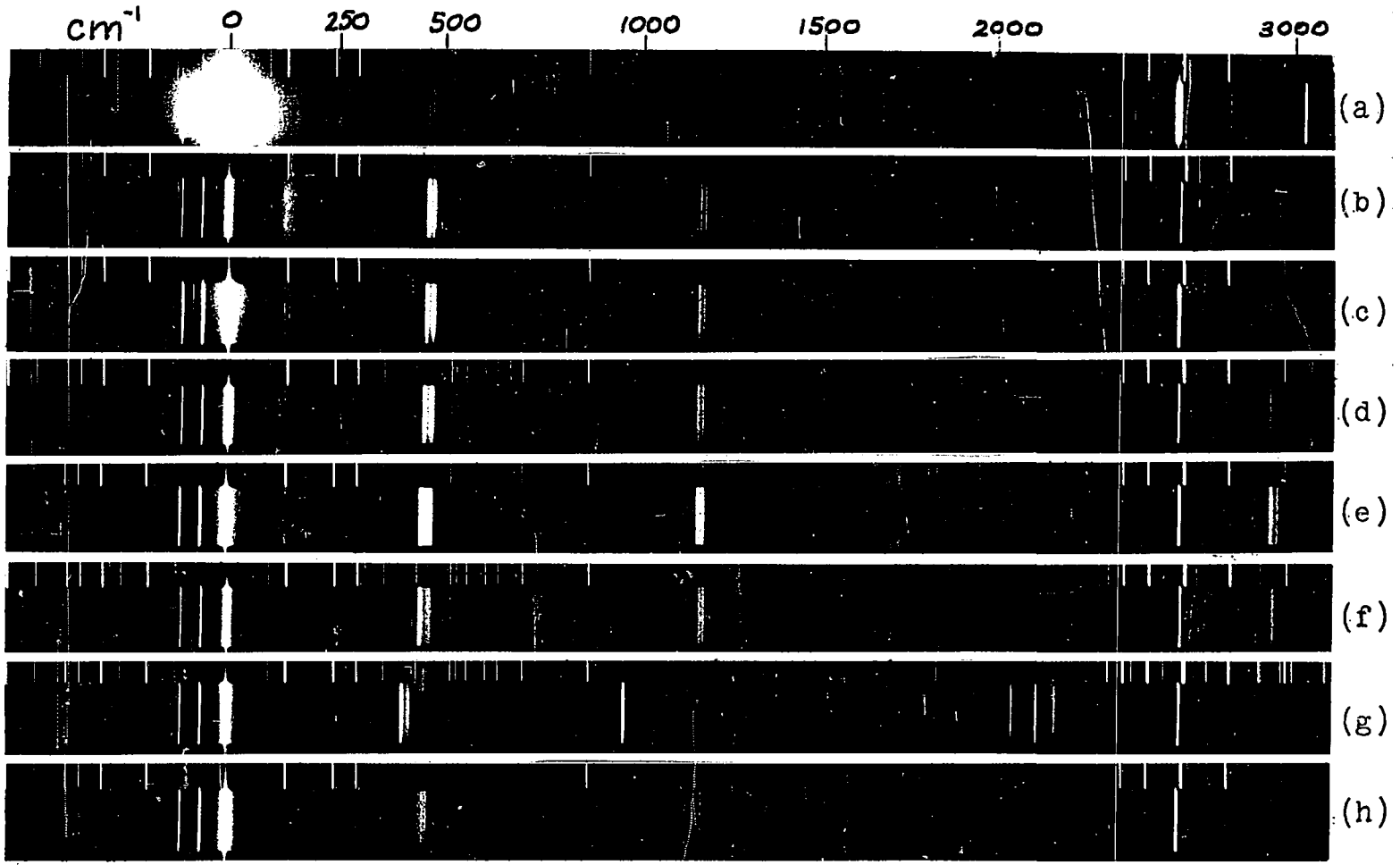

Figure 8. Short Raman Exposures

(a) TML (Crystalline) 20 min -70°C
(b) TML 10 min 10°C
(c) TMEL 30 min - 70°C
(d) DMDEL 1 hr -120°C
(e) MTEL 20 min -100°C
(f) TEL 10 min -120°C
(g) TEL-d_{20} 1 hr -120°C
(h) Triethylbismuth 10 min -125°C

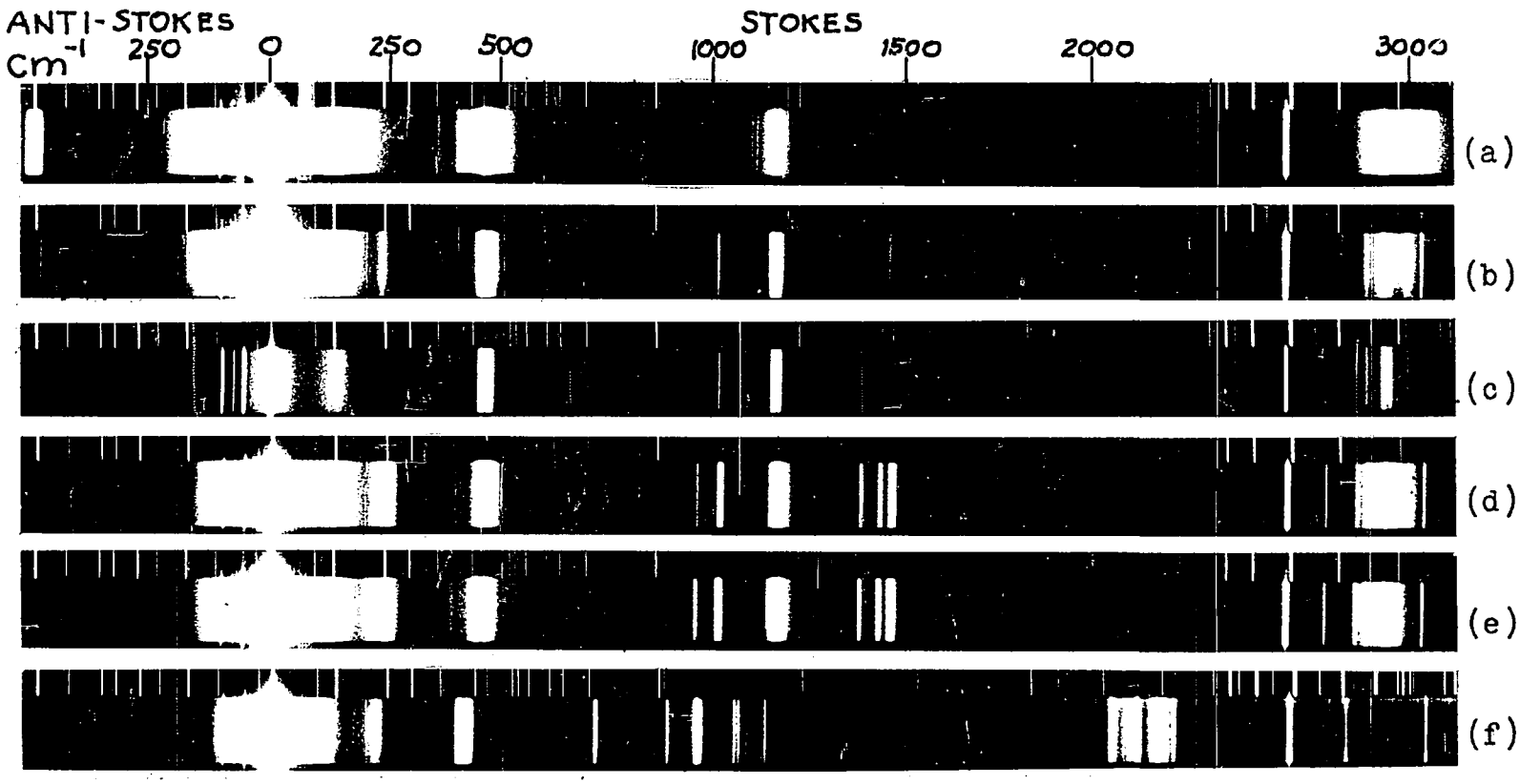

Figure 9. Longest Raman Exposures

(a)	TML	38 hours	10°C
(b)	TMEL	16 hours	- 70°C
(c)	DMDEL	4½ hours	-120°C
(d)	MTEL	13 hours	-100°C
(e)	TEL	18 hours	-120°C
(f)	TEL-d_{20}	26 hours	-120°C

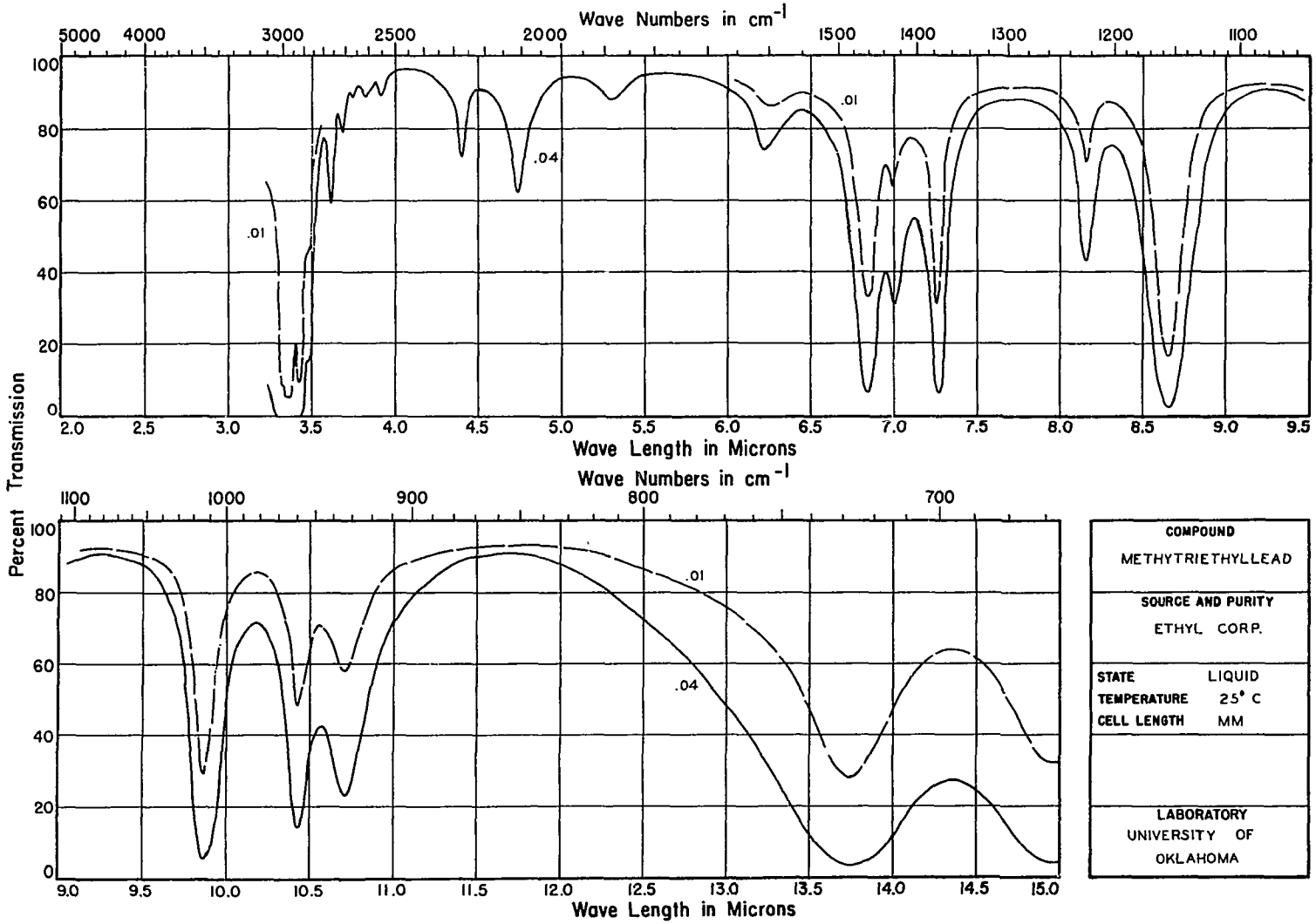

Figure 10. Infrared Spectrum of MTEL
3 to 15 Micron Region

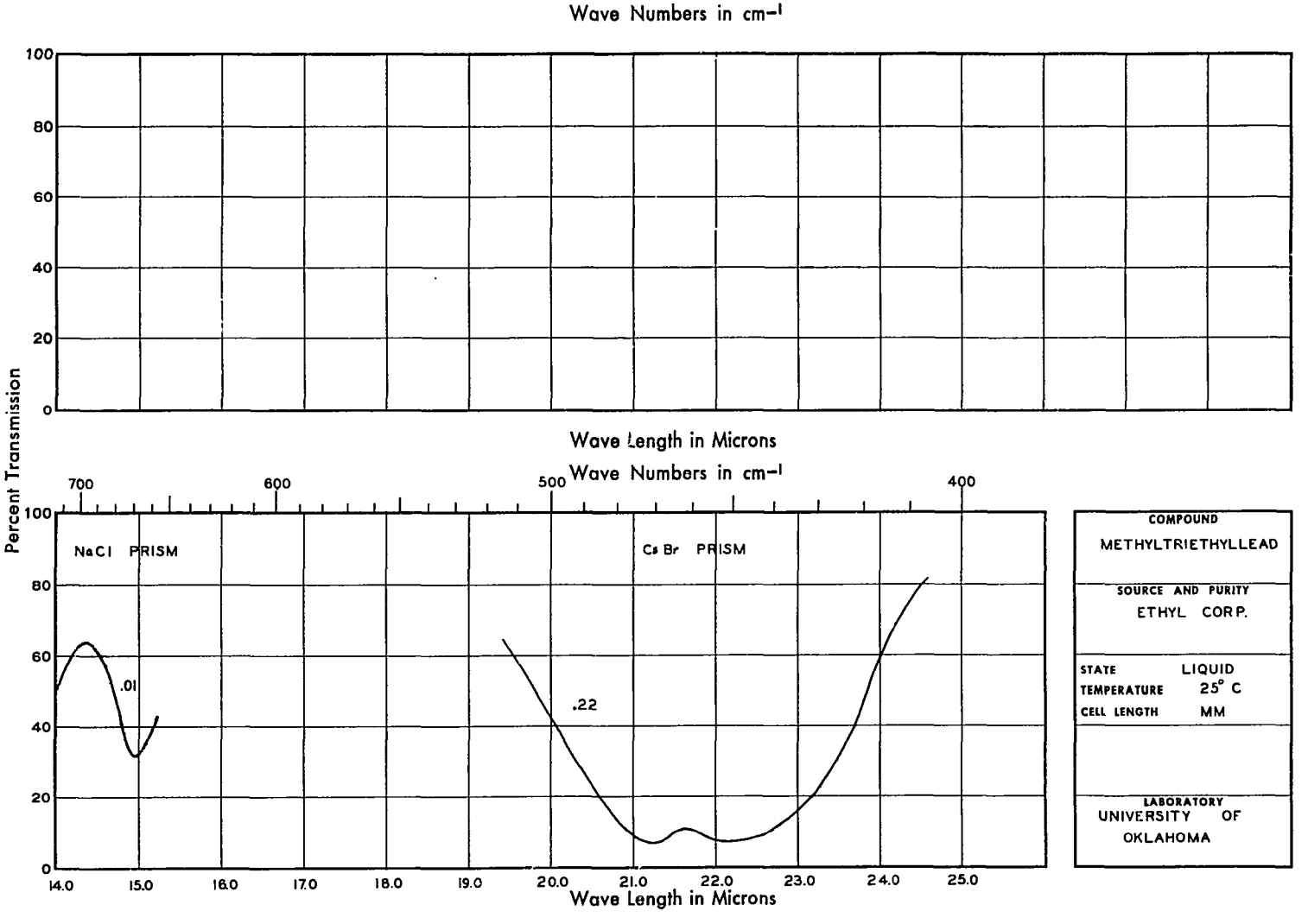

Figure 11. Infrared Spectrum of MTEL
15 to 25 Micron Region

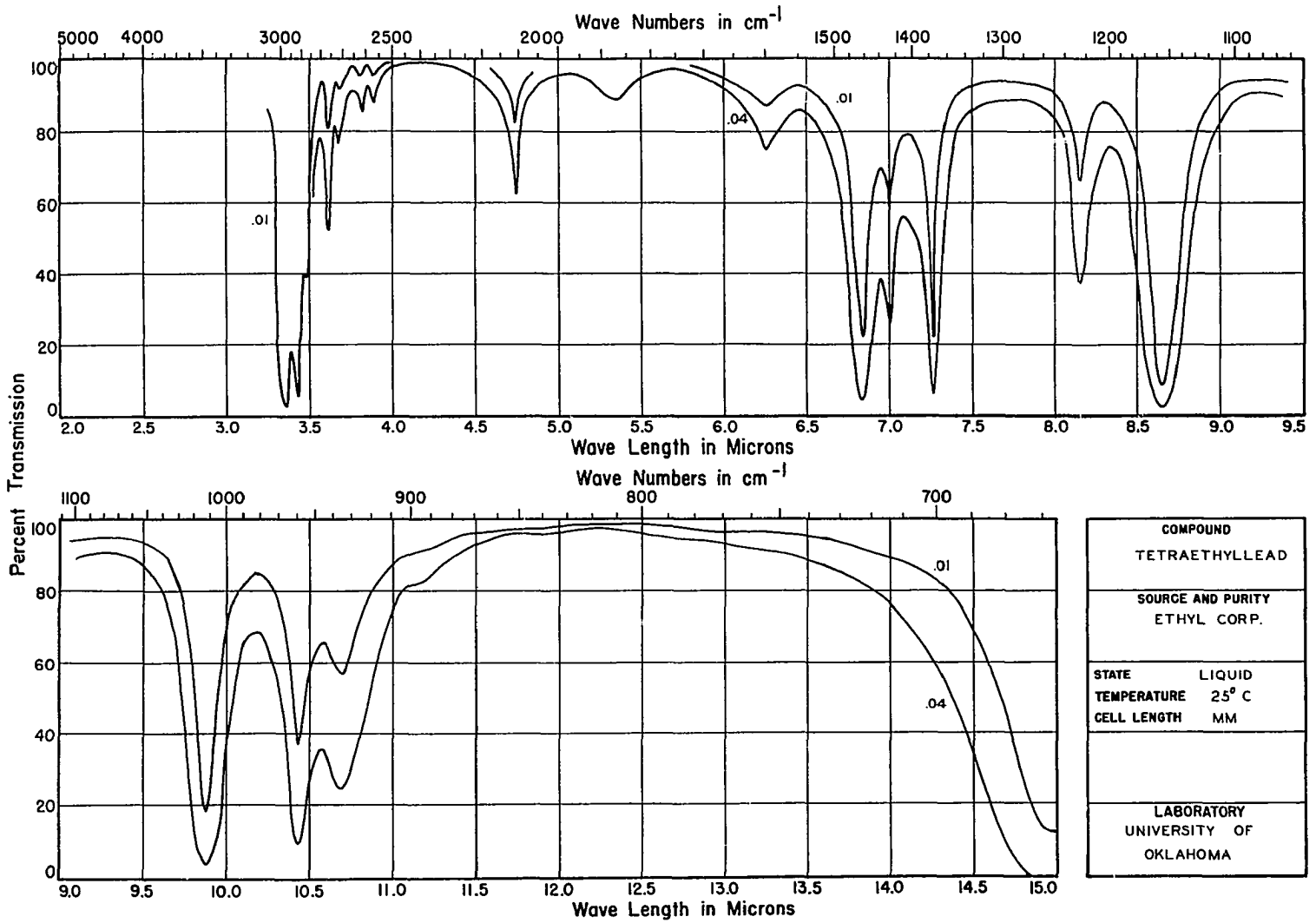

Figure 12. Infrared Spectrum of TEL
3 to 15 Micron Region

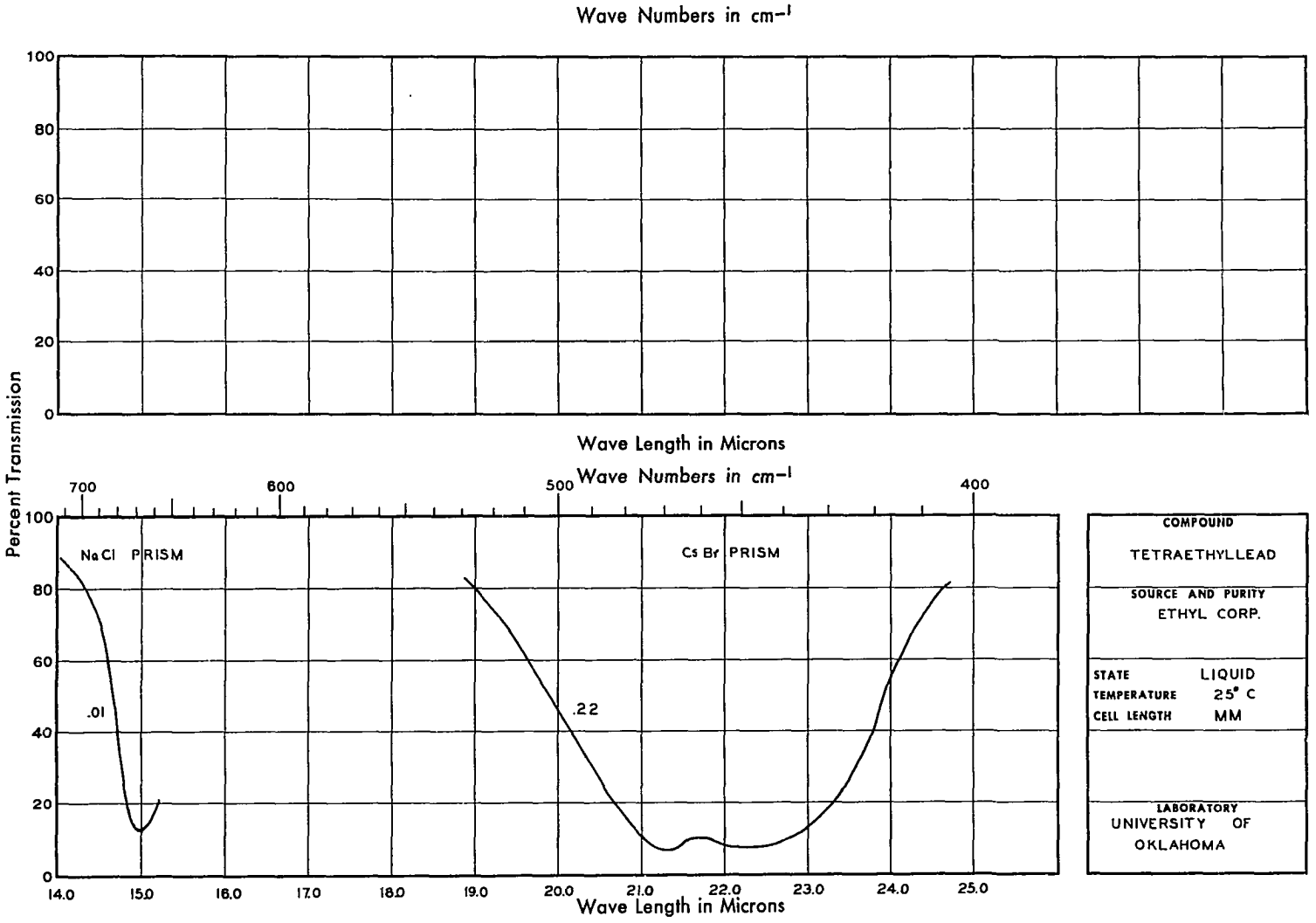

Figure 13. Infrared Spectrum of TEL 15 to 25 Micron Region

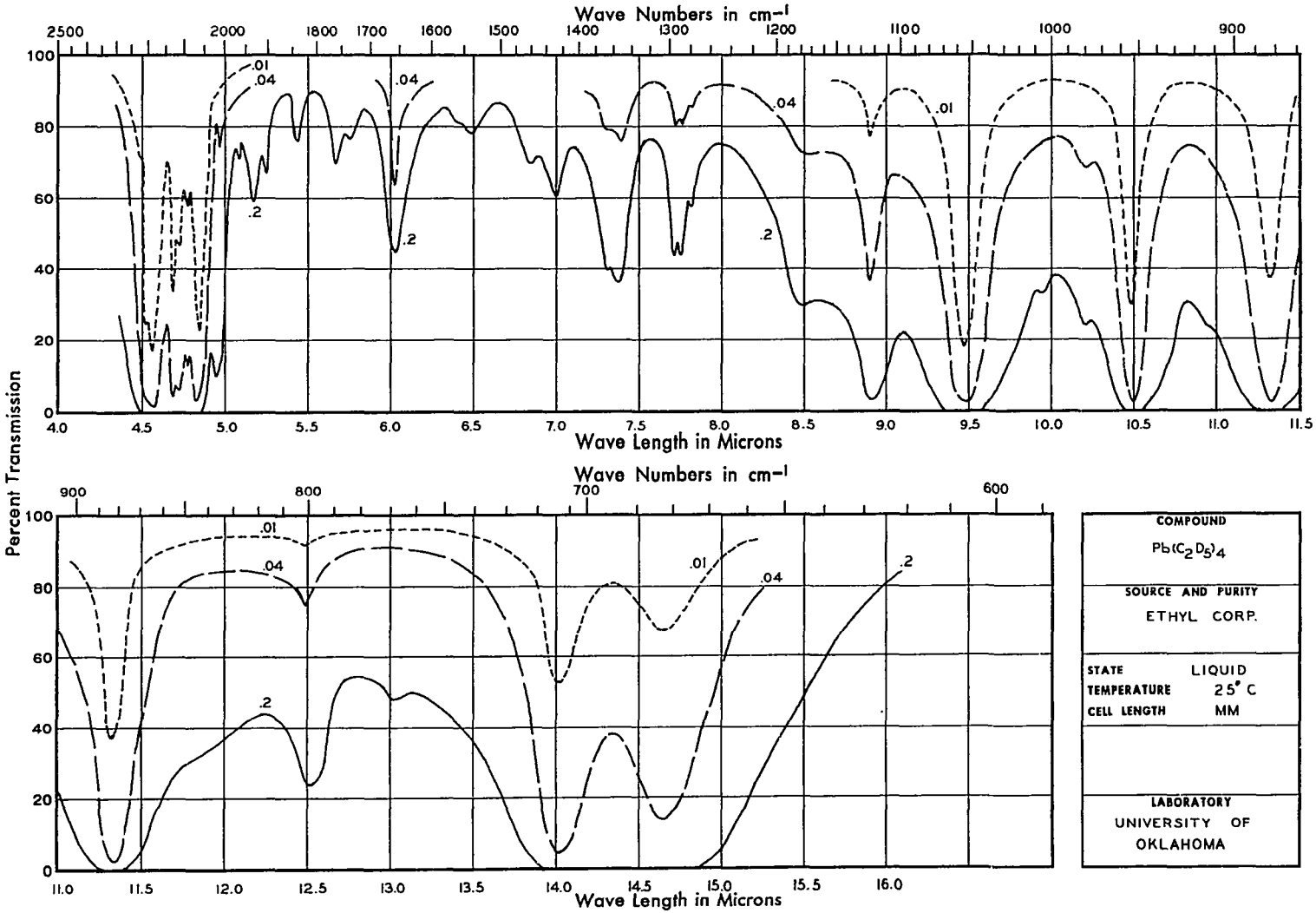

Figure 14. Infrared Spectrum of TEL-d_{20}
3 to 15 Micron Region

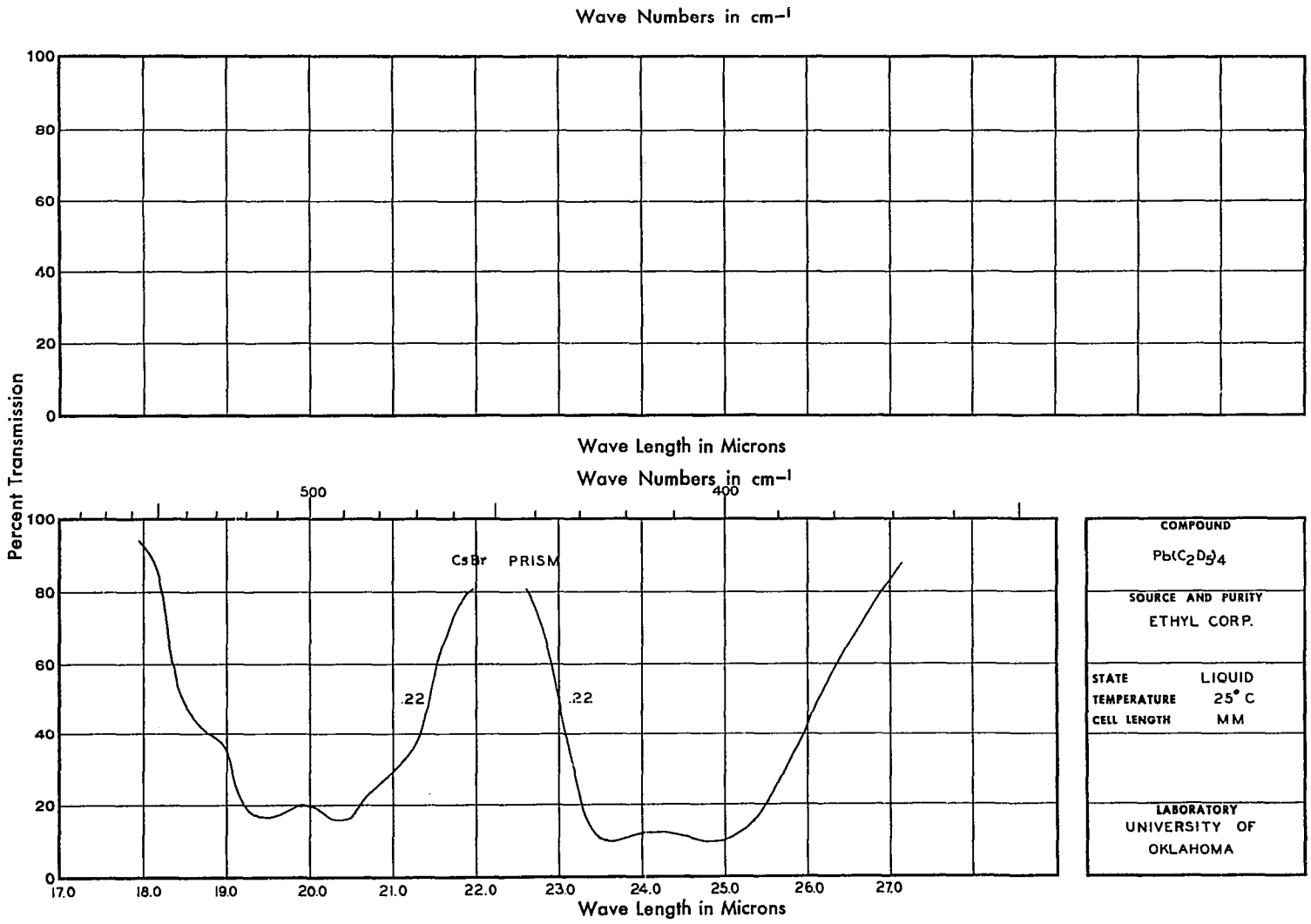

Figure 15. Infrared Spectrum of TEL-d_{20}
15 to 25 Micron Region

TABLE II

RAMAN SPECTRUM OF TETRAMETHYLLEAD (TML)

Wave Number cm^{-1}	Description			Interpretation
130	vs	d	dp	$\nu_{19}(f_2)$
145	vs	d	dp	$\nu_8(e)$
342	vw	b		$212+130=342(A_1+E+F_1+F_2)$*
462	vvs	sh	p	$\nu_3(a_1)$
475	vvs	sh	dp	$\nu_{18}(f_2)$
598	vw	d		$462+130=592(F_2)$ $462+145=607(E)$ $475+130=605(A_1+E+F_1+F_2)$
692	vvvw			$217+475=692(A_2+E+F_1+F_2)$**
769	w	d		$\nu_{17}(f_2)$
~800	w	d		$\nu_7(e)$
~920	vvw	b		$145+769=914(F_1+F_2)$ $2 \times 462=924(A_1)$
1004	vvvw	sh		~800+~200=~1000 $\nu_{11}(f_1)+\nu_{12}(f_1)$ $(A_2+E+F_1+F_2)$ $\nu_{11}(f_1)+\nu_4(a_2)$ (F_2) $\nu_7(e)+\nu_{12}(f_1)$ (F_1+F_2) $\nu_7(e)+\nu_4(a_2)$ (E)
1033	vvw	d		
1157	vs	sh	dp	$\nu_{16}(f_2)$
1169	vs	sh	p	$\nu_2(a_1)$
1286	vw	b		$130+1157=1287(A_1+E+F_1+F_2)$ $145+1157=1302(F_1+F_2)$ $130+1169=1299(F_2)$

TABLE II--Continued

Wave Number cm^{-1}	Description		Interpretation
~1360	vw	b	$1157+215=1372(A_2+E+F_1+F_2)$
1412	w	d	$\nu_6(e)$
1455	w	d	$\nu_{15}(f_2)$
1531	vw	d	$2 \times 769=1538(A_1+E+F_2)$
1622	vw	b	$462+1157=1619(F_2)$ $475+1157=1632(A_1+E+F_1+F_2)$
1644	vw	b	$475+1169=1644(F_2)$
~1833	vvvw		
~1854	vvvw		
1928	vvvw	d	$1455+475=1930(A_1+E+F_1+F_2)$
2096	vvvw	d	
2293	w		$2 \times 1157=2314(A_1+E+F_2)$
2318	vvw	sh	$2 \times 1169=2338(A_1)$
2567	vvvw		$1412+1157=2569(F_1+F_2)$
2918	s	p	$\nu_1(a_1)$, $\nu_{14}(f_2)$
2998	s	dp	$\nu_5(e)$, $\nu_{13}(f_2)$
3706	vvvw	d	$2918+769=3697(E)$

*The band at 342 cm^{-1} may be interpreted as one or more of the sum bands $\nu_4(a_2)+\nu_8(e)$, $\nu_{12}(f_1)+\nu_8(e)$, or $\nu_{12}(f_1)+\nu_{19}(f_2)$. The last combination gives a value of 212 cm^{-1} for $\nu_{12}(f_1)$.

**The band at 692 cm^{-1} is interpreted as the sum band $\nu_{12}(f_1)+\nu_{18}(f_2)$, so that $\nu_{12} \cong 217$ cm^{-1}.

TABLE III

RAMAN SPECTRUM OF CRYSTALLINE TML

Wave Number	Description		Interpretation
155	m		$\nu_8(e)$, $\nu_{19}(f_2)$ skeletal deformation
170	m		
463	vs	sh	$\nu_3(a_1)$ Pb-C stretching
471	s	sh	$\nu_{18}(f_2)$ Pb-C stretching
474	s	sh	
1141	w	sh	$\nu_{16}(f_2)$ sym. CH_3 deformation
1150	w	sh	
1157	vs		$\nu_2(a_1)$ sym. CH_3 deformation
2918	m		$\nu_1(a_1)$, $\nu_{14}(f_2)$ sym. CH_3 stretching
2998	w		$\nu_5(e)$, $\nu_{13}(f_2)$ asym. CH_3 stretching

TABLE IV

RAMAN SPECTRUM OF TRIMETHYLETHYLLEAD (TMEL) (LIQUID)

Wave Number	Description		Interpretation
~135[a]	s	d	skeletal deformation Pb-C-C twisting
235	m		Pb-C-C bending CH_3 torsion
457	vvs	sh	sym. Pb-C stretching
472	vvs		asym. Pb-C stretching
598	vvvw	b	457+135=592
655	vvvw		
683	vvvw		235+457=692
717	vvw	d	CH_2 rocking
763	vw	sh	CH_3 rocking
764	vw	d	CH_3 rocking
917	vvw		2 x 457=914
937	vw		457+472=929 $(CH_3)'$ rocking
960	vw	sh	2 x 472=944 C-C stretching
1017	m	sh	C-C stretching
1154	vs	sh	sym. CH_3 deformation
1166	vs	sh	sym. $(CH_3)'$ def.
1196	vw	sh	CH_2 wagging
1376	w	sh	asym. CH_3 deformation
~1417	vvw	d	asym. $(CH_3)'$ def.

TABLE IV--Continued

Wave Number	Description		Interpretation
1427	w	sh	CH_2 deformation
1458[b]			
1620	vvvw		472+1154=1626 457+1166=1623
1690	vvvw		235+1458=1693
1880	vvvw		457+1427=1884
2023	vvvw		2 x 1017=2034
2165	vvw		1017+1154=2171
2190	vvvw		1017+1166=2183
2290	vw	sh	2 x 1154=2308
2311	vvvw		2 x 1166=2332 1166+1154=2320
2468	vvvw		1456+1017=2473
2495	vvw		
2560	vvw	b	
2650	vvw		
2684	vvw		
2729	vw	sh	2 x 1376=2752
2833	vw		
2864			2 x 1427=2854 1376+1458=2834
2901[c]	m		sym. CH_2 stretching 1427+1458=2885
2920	s	sh	sym. CH_3 stretching 2 x 1458=2916
2939	m		sym. $(CH_3)'$ stretching

TABLE IV--Continued

Wave Number	Description		Interpretation
2964[d]	w	d	asym $(CH_3)'$ str.
2997	m		asym. CH_3 stretching
3124	vvw		
3481	vvvw		
3496	vvvw		
3723	vvvw		

[a]Strong exposure shows three weak, sharp bands at 127, 134, and 144 cm^{-1} superposed on strong diffuse band with center at approximately 135 cm^{-1}.

[b]May be double.

[c]Right edge obscured by band at 2920 cm^{-1}.

[d]$(CH_3)'$= methyl group not bonded directly to lead atom.

TABLE V

RAMAN SPECTRUM OF DIMETHYLDIETHYLLEAD (DMDEL) (LIQUID)

Wave Number	Description		Interpretation
~132	s	d	skeletal deformation Pb-C-C twisting
229	vw	b	CH_3 torsion Pb-C-C bending
242	w	d	Pb-C-C bending
449	vvs	sh	sym. Pb-C stretching
469	vvs	b	asym. Pb-C stretching
959[a]	vvw	sh	$(CH_3)'$ rocking C-C stretching
1016	m	sh	C-C stretching
1153	vs	sh	sym. $(CH_3)'$ def.
1166	vs	sh	sym. CH_3 def.
1374	w	sh	asym. $(CH_3)'$ def.
1427	w	sh	asym. CH_3 def. CH_2 def.
1457[b]	w		
1864	vvvw		449+1427=1876
1934	vvvw		469+1457=1926
2726	vvw	sh	2 x 1374=2748
2785	vvvw		1374+1427=2801
2828	vvw		1374+1427=2831
2860	m	sh	sym. CH_2 stretching
2896	vw		2 x 1427=2854 1427+1457=2884
2918	s	sh	2 x 1457=2914

TABLE V--Continued

Wave Number	Description	Interpretation
2940	m sh	sym. CH_3 stretching
2964	vw	sym. $(CH_3)'$ stretching
2996	w d	asym. CH_3 stretching asym. $(CH_3)'$ str.

[a] $(CH_3)'$ = methyl group not bonded directly to lead atom.

[b] May be double.

TABLE VI

RAMAN SPECTRUM OF METHYLTRIETHYLLEAD (MTEL) (LIQUID)

Wave Number	Description			Interpretation
60	m	sh		
~128	s	d	dp	skeletal deformation Pb-C-C twisting
225	w	b		Pb-C-C bending
241	m	d		CH_3 torsion
446	vvs	sh	p	sym. Pb-C stretching
466[a]	vs		dp	asym. Pb-C stretching
~565	vvvw	d		128+446=574
~585	vvvw	d		128+466=594
641	vvvw			CH_2 rocking
661	vvvw			225+446=671
677	vvw	sh		
713	vvvw			241+466=707
728	vw			CH_3 rocking CH_2 rocking
916	vw	d		446+466=912
936	vw	sh		2 x 466=932 $(CH_3)'$ rocking C-C stretching
958	w	sh		225+728=953
1003[b]	vw			
1015	s	sh		C-C stretching
1152	vs	sh	dp	sym. CH_3 stretching
1163	vw	sh	p	sym. $(CH_3)'$ str.

TABLE VI--Continued

Wave Number	Description		Interpretation
1197[c]	vw		466+728=1194
1225	vw	sh	CH_2 wagging
1279	vvvw	d	128+1152=1280
1318[d]	vvvw		
1374	m	sh	asym. $(CH_3)'$ def.
~1400[e]	vw	b	asym. CH_3 def.
1425	m	sh	225+1152=1377 225+1163=1388 241+1152=1393 241+1163=1404 446+958=1404 466+958=1424 446+1015=1461
1456	m	sh	CH_2 def.
1609	vvw	d	446+1163=1609 241+1374=1611
1682	vvvw	d	225+1456=1681 728+958=1686
1862	vvvw	d	446+1425=1871
1916	vvvw	d	466+1456=1922
1970	vvvw	d	958+1015=1973
2018	vw	sh	2 x 1015=2030
2050	vvvw	d	677+1374=2051
2073	vvvw	d	916+1163=2079
2095	vw	d	936+1163=2099 958+1152=2110
2234	vvvw	d	
2276	vvw	sh	916-1374=2290

TABLE VI--Continued

Wave Number	Description			Interpretation
2308	vvw			2 x 1152=2304 936+1374=2310 1152+1163=2315
2329	vvw			2 x 1163=2326 958+1374=2332
2383	vvw	sh		958+1425=2383 1015+1374=2389
2408	vvvw	sh		958+1456=2414
2489	vvvw			1015+1456=2471
2533	vvw	b		1163+1374=2537 1152+1374=2526
2556	vvvw	sh		1152+1425=2577
2644	vvw	sh		
2679	vvw	sh		
2725	w	sh		2 x 1374=2748
2829	w	sh		1374+1456=2830
2860	s	sh	p	2 x 1425=2850 sym. CH_2 stretching
2895	m	sh		1425+1456=2881
2915	vs	sh	p	2 x 1456=2912 sym. CH_3 stretching
2939	s	sh		sym. $(CH_3)'$ str. asym. CH_2 stretching
2965	m	sh		asym $(CH_3)'$ str. asym. CH_3 stretching
2995	w	b		
3619	vvvw	d		728+2895=3623
3693	vvvw	d		958+2725=3683
3723	vvvw	d		1015+2725=3740

TABLE VI--Continued

Wave Number	Description	Interpretation
3829	vvvw d	1015+2829=3844

[a]May be double.

[b]Right edge obscured by band at 1015 cm^{-1}.

[c]Left edge obscured by band at 1163 cm^{-1}.

[d]Not believed to be band at 1374 cm^{-1} excited by mercury "f" line.

[e]Right edge obscured by bands at 1425 and 1456 cm^{-1}.

TABLE VII

RAMAN SPECTRUM OF TETRAETHYLLEAD (TEL) (LIQUID)

Wave Number	Description			Interpretation
~107	s	d	dp	skeletal deformation Pb-C-C twisting
213	w	d		$(CH_3)'$ torsion Pb-C-C bending
243	m	d		Pb-C-C bending
443	vvs	sh	p	sym. $(Pb-C)'$ str.
~461[a]	vs	b	dp	asym. $(Pb-C)'$ str.
641	vvvw			
657	vvvw			213+443=656
674	vvw	sh		CH_2 rocking 213+461=674
905	vvw	d		443+461=904
928[b]	vw	sh		$(CH_3)'$ rocking
936[b]	vw	sh		2 x 461=922
958	w	sh		$(CH_3)'$ rocking C-C stretching
999[c]	vw			
1014	s	sh		C-C stretching
1155	vs	sh	dp	sym. $(CH_3)'$ def.
1164	vs	sh	p	sym. $(CH_3)'$ def.
1225	vw	sh		CH_2 wagging 213+1014=1227
1254	vvvw			243+1014=1257

TABLE VII--Continued

Wave Number	Description		Interpretation
1276	vvvw		107+1164=1271
1319	vvvw	sh	
1373	m	sh	asym. $(CH_3)'$ def. CH_2 def.
~1400[d]	vw	b	
1424	m	sh	
1458[e]	m	sh	
1604	vw	d	443+1164=1607
1686	vvw	b	243+1458=1701
1787	vvvw		
1859	vvw	d	443+1424=1867
1891	vvvw		443+1458=1901 936+958=1894
1919	vvvw		2 x 958=1916 458+1462=1920
1976	vvvw		958+1014=1972
2016	vw	sh	2 x 1014=2028
2027	vvw		
2073	vvvw	d	
2092	vw	d	936+1164=2100
2096	vw	sh	958+1155=2113
2243	vvvw		
2305	vvw	sh	2 x 1155=2310 936+1373=2309

TABLE VII--Continued

Wave Number	Description			Interpretation
2326	vvw	sh		1155+1164=2319 2 x 1164=2328
2380	vvw	sh		958+1424=2382 1014+1373=2387
2406	vvvw	sh		958+1458=2416
2431	vvvw			1014+1424=2432
2471	vvvw			1014+1458=2472
2535	vvw			1164+1373=2537
2557	vvw			
2641	vw			
2667	vw			
2723	w	sh		2 x 1373=2746
2803[f]	vw			
2824	w	sh		
2860	s	sh		asym. CH_2 stretching 1373+1458=2831 2 x 1424=2848 sym. CH_2 stretching 1424+1458=2882 sym. $(CH_3)'$ stretching 2 x 1458=2916 asym. $(CH_3)'$ str.
2895	m	sh		
2918	s	sh	p	
2940	s	sh		
2960	m	sh		
3167	vvw	b		2918+243=3161 2960+213=3173
3503	vvvw			2824+674=3498
3599	vvvw	d		2918+674=3592

TABLE VII--Continued

Wave Number	Description	Interpretation
3680	vvw sh	

[a]May be double.

[b]Not fully resolved.

[c]Right edge obscured by band at 1014 cm^{-1}.

[d]Right edge obscured by band at 1458.

[e]May be double.

[f]Right edge obscured by band at 2824 cm^{-1}.

TABLE VIII

RAMAN SPECTRUM OF $Pb(C_2D_5)_4$ (TEL-d_{20}) (LIQUID)

Wave Number	Description		Interpretation
~95	s	d	skeletal deformation
169	vw		Pb-C-C bending
196	vw		CH_3 torsion
217	m	d	CH_3 torsion
401	vs	sh	sym. Pb-C stretching
416	vs		asym. Pb-C stretching
484	vw		CD_2 rocking 95+401=496 95+416=511
497	vw		CD_2 rocking 95+401=496 95+416=511
509	vw		CD_2 rocking 95+401=496 95+416=511
543	vvvw		fundamental?
672	vw		CD_3 rocking 169+509=678 196+484=680 196+497=693
683	vw		CD_3 rocking 169+509=678 196+484=680 196+497=693
710	m		CD_3 rocking C-C stretching 217+497=714
767	vw	sh	fundamental? 95+672=767
801	vw		95+710=805 2 x 401=802
819	vw		401+416=817 2 x 416=832
883	m	sh	C-C stretching 401+484=885

TABLE VIII--Continued

Wave Number	Description		Interpretation
940	w	sh	sym. CD_3 def. 401+543=944
955	vvs	sh	sym. CD_3 def. 416+453=959
~966[a]			2 x 484=968
982	w	sh	CD_2 wagging
1047	m	sh	
1058	m	sh	asym. CD_3 def. CD_2 def. 95+955=1050 401+710=1111 169+955=1124
1104	vw	sh	
1113	vw	sh	
1124	m	sh	
1224	vvvw		543+683=1226 169+1058=1227
1289	vvw	d	416+883=1299 169+1124=1293
1354	vvw	d	401+955=1356
1375	vvw		2 x 683=1366 416+955=1371 497+883=1380
1420	vvvw		2 x 710=1420 484+940=1424
1629	vvw		672+955=1627 543+1124=1633
1661	vvw		710+955=1665
1762	vvw		2 x 883=1766 710+1058=1768

TABLE VIII--Continued

Wave Number	Description	Interpretation
1836	vvw	710+1124=1834 883+955=1838
1869	vvw	2 x 940=1880
1900	w sh	2 x 955=1910
1928	vvw	883+1047=1930 883+1058=1941
1959	vvw	
1999	w	940+1058=1998 955+1047=2002
2014	w	955+1058=2013
2061	vs sh	C-D stretching 940+1124=2064
2073	w	955+1124=2079
2099	w	1047+1058=2105
2120	w sh	2 x 1058=2116
2139	vs sh	sym. CD_2 stretching 1058+1124=2182
2183	m sh	sym. CD_2 stretching
2197	s sh	asym. CD_2 stretching
2207	m sh	asym. CD_3 stretching
2223	m sh	2 x 1124=2248
2247	m sh	

[a]Left edge obscured by band at 955 cm^{-1}.

TABLE IX

RAMAN SPECTRUM OF TRIETHYLBISMUTH (LIQUID)

Wave Number	Description		Interpretation
~124	vw	d	skeletal deformation
~160	vw	d	Bi-C-C twisting
~213	vw		Bi-C-C bending
~228	vw		CH_3 torsion
~253	w	d	
440	vs	sh	Bi-C stretching
451	vs	sh	
461	vs	sh	
~955	vw		CH_3 rocking C-C stretching
1018	w	b	
1149	s	b	sym. CH_3 deformation
1163	s	sh	
1371	w		CH_2 deformation
1422	w		asym. CH_3 deformation
1454	w	b	
2825	vw		C-H stretching
2860	m	sh	
2891	w	sh	
2912	m	sh	
2937	m	sh	
2958	vw		

TABLE X

INFRARED SPECTRUM OF METHYLTRIETHYLLEAD (MTEL) (LIQUID)

Wave Number	Description		Interpretation
446	vs		sym. Pb-C stretching
466	vs		asym. Pb-C stretching
662	s		CH_2 rocking 225+446=671 241+446=687
670	s	b	
727	vvs	b	CH_3 rocking CH_2 rocking
934	s	b	2 x 466=932 $(CH_3)'$ rocking C-C stretching
959	s	sh	
1014	vs	sh	C-C stretching
1155	vvs	sh	sym. CH_3 stretching
1228	m	sh	CH_2 wagging
1375	vs	sh	asym. $(CH_3)'$ def. asym. CH_3 def. 446+959=1405 466+959=1425 446+1014=1460 CH_2 def.
1428	m	sh	
1459	vs	sh	
1606	vw	b	446+1163=1609 241+1375=1612
1890	vw	b	466+1425=1891
2110	w	sh	959+1155=2114
2275	vw	sh	916+1375=2291
2464	vvvw		1015+1459=2474
2561	vvw		1155+1428=2583
2610	vvw		1163+1459=2622

TABLE X--Continued

Wave Number	Description	Interpretation
2677	vvvw	
2717	vvw sh	
2768	vw sh	2 x 1375=2750
2878	m sh	C-H stretchings
2939	s sh	
3195	vvvw	

TABLE XI

INFRARED SPECTRUM OF TETRAETHYLLEAD (TEL) (LIQUID)

Wave Number	Description		Interpretation
445	s		sym. Pb-C stretching
467	s		asym. Pb-C stretching
667	vs	d	CH_2 rocking
936	s		CH_3 rocking 2 x 467=934
959	vs	sh	CH_3 rocking C-C stretching
1013	vs	sh	C-C stretching
1154	vvs	sh	sym. CH_3 deformation
1227	m	sh	CH_2 wagging
1377	vs	sh	asym. CH_3 deformation
1427	m		CH_2 deformation
1460	vs	sh	
1599	vw		445+1154=1599
1890	vw		445+1460=1905 936+959=1895
2110	w	sh	959+1154=2113
2567	vvw		1154+1427=2581
2611	vvw		1154+1460=2614
2729	vvw		2 x 1377=2754
2762	vw		1373+1424=2797
2878	s		C-H stretching
2910	s		

TABLE XII

INFRARED SPECTRUM OF $Pb(C_2D_5)_4$ (TEL-d_{20}) (LIQUID)

Wave Number	Description	Interpretation
400	vs	sym. Pb-C stretching
425	vs	asym. Pb-C stretching
480	s	
495	s	CD_2 rocking 95+400=495 95+425=520
512	s	
537	s	
683	s	CD_3 rocking 169+512=681
713	s	CD_3 rocking C-C stretching 217+495=712
768	vw	fundamental? 95+672=767
800	w	95+713=805 2 x 400=800
883	vs	C-C stretching 400+480=880
915	vvw	sym. CD_3 deformation
954	vs	
982	vw	CD_2 wagging
1006	vvw	495+512=1007
1047	vs	95+954=1049 asym. CD_3 def. CD_2 deformation 400+713=1113 169+954=1123
1056	vs	
1116	vvvw	
1124	m	

TABLE XII--Continued

Wave Number	Description	Interpretation
1180	w	495+683=1178
1218	vvvw	543+683=1226 169+1056=1225
1279	vw	512+768=1280
1289	w	400+883=1283
1297	w	169+1124=1293
1306	vw	425+883=1308
1356	w	672+683=1355
1367	w	2 x 683=1366
1428	vw	2 x 713=1426
1462	vw	512+954=1466
1544	vw	425+1124=1549
1627	vvvw	683+954=1637
1664	m	713+954=1667
1765	vw	768+954=1772 713+1056=1769
1840	vw	713+1124=1837 883+954=1837
1907	vw	2 x 954=1908
1934	vw	
1944	vw	883+1056=1939
1990	vw	954+1047=2001
2015	m	954+1056=2010

TABLE XII--Continued

Wave Number	Description	Interpretation
2064	vs	C-D stretching 954+1124=2078
2094	m	1047+1056=2103
2123	s	2 x 1056=2112
2139	s	sym. CD_2 stretching 1056+1124=2180 sym. CD_3 stretching asym. CD_2 stretching asym. CD_3 stretching 2 x 1124=2248
2183	s	
2200	vs	
2223	vs	
2249	m	

CHAPTER V

POSSIBLE MOLECULAR SYMMETRIES

Introduction

The analysis of the observed spectra is complicated by the fact that for all the lead alkyls, except TML, there are several possible configurations of the lead-carbon skeleton. In the following paragraphs these different configurations are discussed.

Under the assumption that the entire molecule has the same symmetry as the lead-carbon skeleton, the distribution of the normal vibrations among the various symmetry species is given in tabular form. This assumption will be valid if all methyl groups are either "eclipsed" or "staggered," and in some cases for other orientations of the methyl groups, but it will not hold for arbitrary orientations of the methyl groups.

In addition to the possibilities listed, all lead-carbon skeletons and all molecules may have the symmetry C_1, i.e., have no symmetry.

Possible Symmetry of TML

In TML, the four carbon atoms are probably arranged

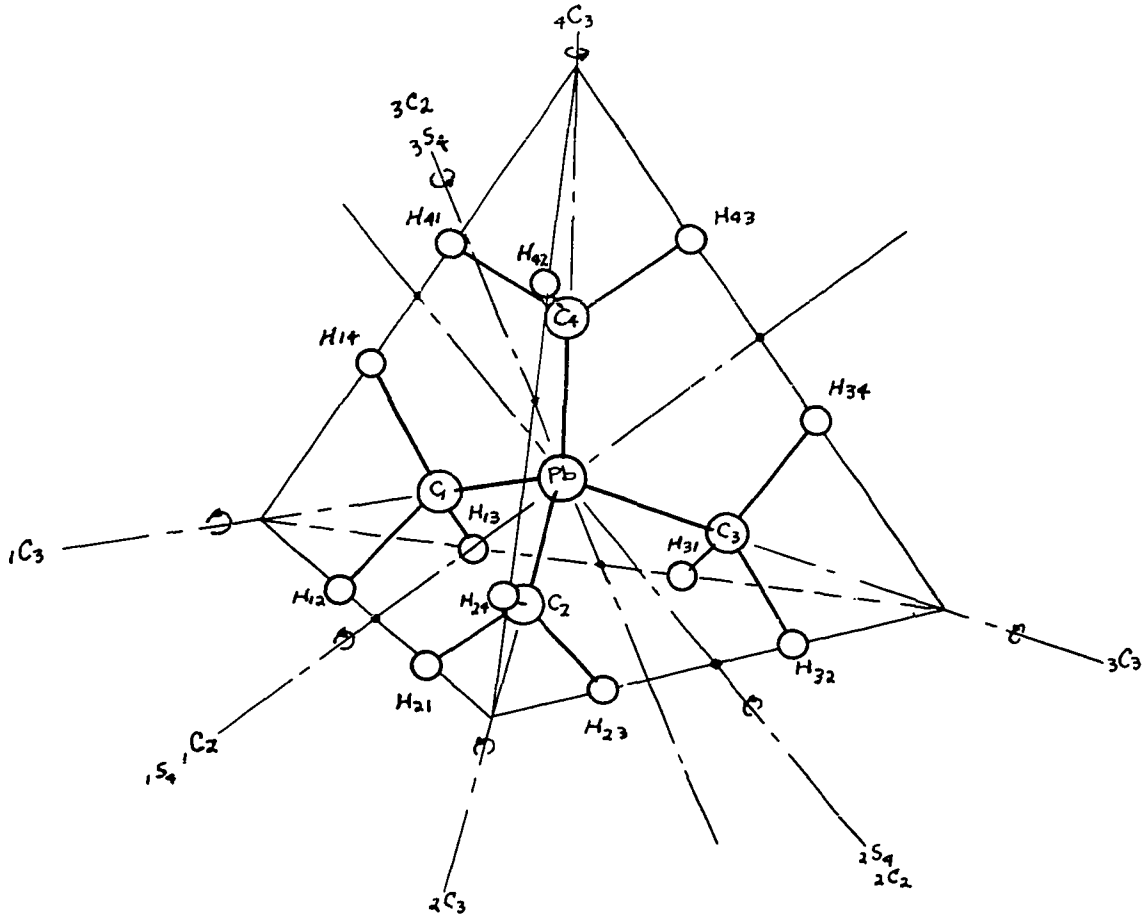

TETRAMETHYLLEAD IN ECLIPSED CONFIGURATION

Fig. 16

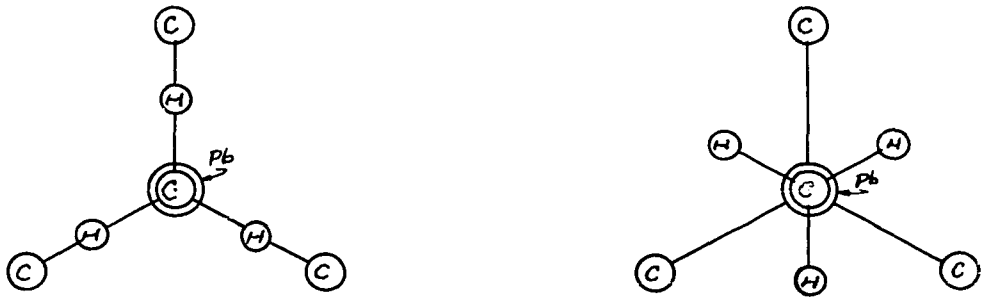

ORIENTATION OF METHYL GROUPS IN (a) ECLIPSED AND (b) STAGGERED CONFIGURATIONS

Fig. 17

about the lead atom so that they fall at the corners of a regular tetrahedron with the lead atom at the center.

There are two possible configurations of the methyl group, the "eclipsed" and the "staggered," in which TML will have the symmetry T_d. In the former, the C-H bonds in a particular methyl group "eclipse" the Pb-C bonds when the molecule is viewed along the Pb-C bond associated with the methyl group considered. In the latter configuration, the C-H and Pb-C bonds are "staggered" 60°. These configurations are shown in Figs. 17(a) and 17(b), page 69. It is possible that the methyl groups are neither eclipsed nor staggered. This possibility is unlikely, however, and will not be considered further.

If the TML molecule has the symmetry T_d, its 45 normal vibrations are distributed among the various symmetry species for this point group as follows: $3a_1 + a_2 + 4e + 4f_1 + 7f_2$. The a_1, e, and f_2 vibrations are active in the Raman effect, while only the f_2 vibrations are infrared active. There should, therefore, be 14 fundamentals observable in the Raman effect and 7 observable in the infrared spectrum.

The distribution of the normal vibrations of different character among the various symmetry species is given in Table XVII, page 87 . The characterization of the normal vibrations by a single type of motion is only approximate, since they will generally consist of a mixture of these different motions. The motion listed is that of which the

vibration is largely composed.

Possible Symmetry of TMEL

The most symmetric configuration of TMEL has one plane of symmetry and belongs to the point group C_s. There are two possible configurations of the lead-carbon skeleton that have this symmetry. These are illustrated in Plate I, Figs. 1(a) and 1(b), page 72. For each of them there are an infinite number of possible orientations of the methyl groups for which the molecular symmetry is unchanged, since the methyl groups, whose carbon atoms are on the plane of symmetry, can be either staggered or eclipsed, and the other two methyl groups can assume arbitrary orientations, provided they are mirror images of each other with respect to the plane of symmetry. Even if only eclipsed or staggered orientations of the methyl groups are considered, there are several configurations of symmetry C_s.

The division of the 54 normal vibrations between the two species a' and a" is given in Table XIII, page 73. Vibrations of both species a' and a" are active in both Raman and infrared. There should, therefore, be 54 fundamental bands observable in both Raman and infrared spectra. However, many of these will overlap, so that the number of observed frequencies is greatly reduced.

Possible Symmetry of DMDEL

The lead-carbon skeleton can, at most, have the

PLATE I

POSSIBLE CONFIGURATIONS OF
LEAD-CARBON SKELETON IN TMEL

C_s

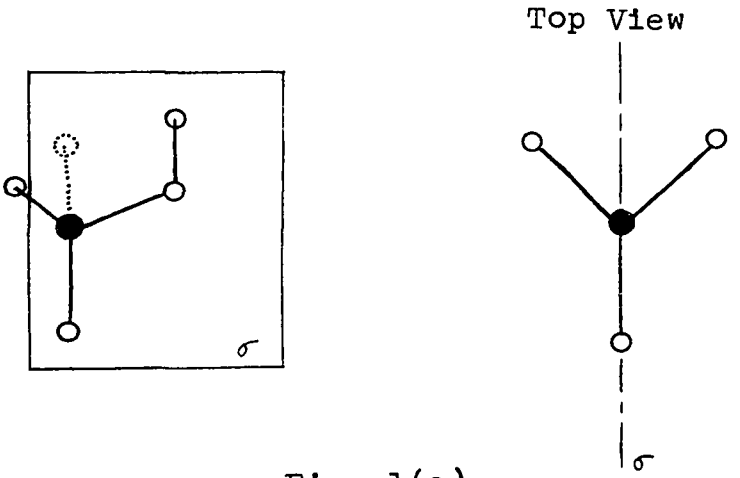

Fig. 1(a)

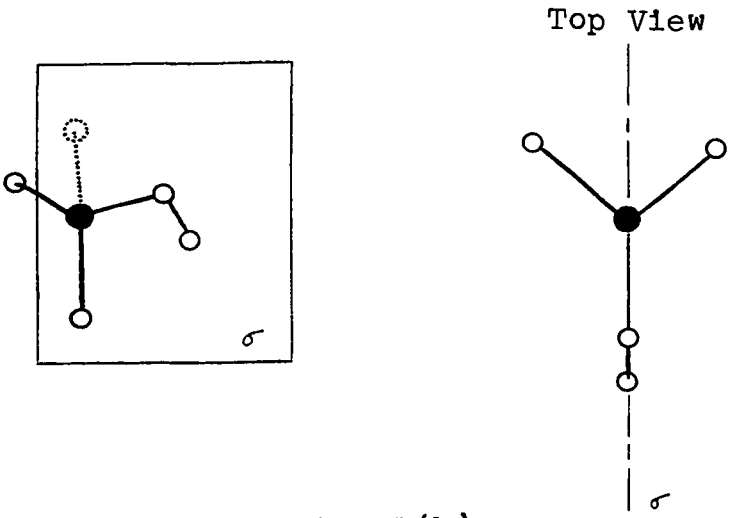

Fig. 1(b)

Legend

● Lead

○ Carbon

TABLE XIII

CLASSIFICATION OF THE FIFTY-FOUR NORMAL VIBRATIONS OF TMEL FOR THE SYMMETRY C_s[a]

Approximate Character	C_s	
	*a'+	*a"+
Methyl		
$(CH_3)'$ asym. str.	1	1
CH_3 asym. str.	3	3
$(CH_3)'$ sym. str.	1	0
CH_3 sym. str.	2	1
$(CH_3)'$ asym. def.	1	1
CH_3 asym. def.	3	3
$(CH_3)'$ sym. def.	1	0
CH_3 sym. def.	2	1
$(CH_3)'$ rocking	1	1
CH_3 rocking	3	3
$(CH_3)'$ torsion	0	1
CH_3 torsion	1	2
Methylene		
CH_2 asym. stretching	0	1
CH_2 sym. stretching	1	0
CH_2 deformation	1	0
CH_2 wagging	1	0
CH_2 twisting	0	1
CH_2 rocking	0	1
Skeletal		
C-C stretching	1	0
Pb-C stretching	2	1
(Pb-C)' stretching	1	0
Pb-C-C bending	1	0
Pb-C-C twisting	0	1
C-Pb-C deformation	3	2
Total	30	24

[a] $(CH_3)'$ = methyl group not bonded directly to lead atom; (Pb-C)' = lead-carbon bond between lead atom and methylene group; * = Raman active; + = infrared active.

symmetry C_{2v}. Two configurations with this symmetry are possible. These are illustrated diagramatically in Plate II, Figs. 1(a) and 1(b), page 75.

If each ethyl group is rotated about the Pb-C bond through an angle $\phi(\neq 0^\circ, \neq 180^\circ)$ in the same sense when viewed along the bond, as shown in Plate II, Fig. 2, the molecule will have the symmetry C_2. Since ϕ is arbitrary, there are an infinite number of possible configurations with this symmetry.

If the two ethyl groups are rotated in the opposite sense through an angle $\phi(\neq 0^\circ, \neq 180^\circ)$ as shown in Plate II, Fig. 3, the molecule will have the symmetry C_s. Since ϕ is arbitrary, there will be an infinite number of these configurations in which the two ethyl groups are mirror images of each other with respect to the plane of symmetry.

If one of the ethyl groups is rotated through an angle $\phi = 180^\circ$ and the other unchanged ($\phi = 0^\circ$) the molecule will again have the symmetry C_s, but with the symmetry plane as shown in Plate II, Fig. 4, so that the two methyl groups form mirror images of each other. There is only one such configuration for the lead-carbon skeleton.

The distribution of the 63 normal vibrations among the symmetry species is given in Table XIV, page 76. In this table $C_s(a)$ and $C_s(b)$ refer to the configurations shown in Plate II, Figs. 3 and 4, respectively.

PLATE II

POSSIBLE CONFIGURATIONS OF
LEAD-CARBON SKELETON IN DMDEL

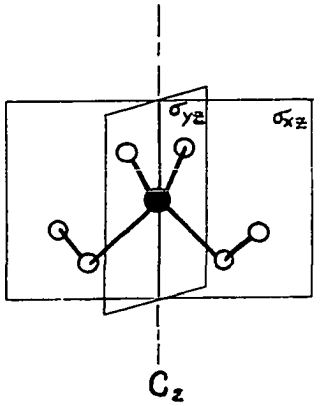

Fig. 1(a)

C_{2v}

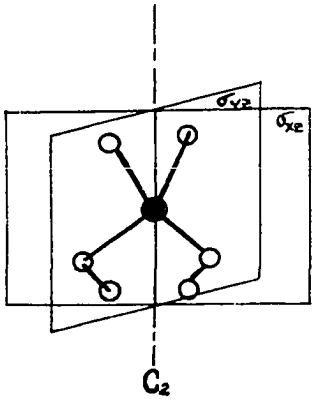

Fig. 1(b)

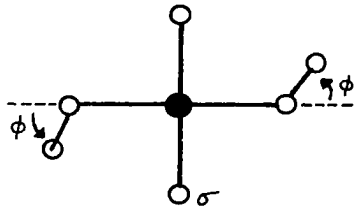

Fig. 2(a).--Top View

C_2

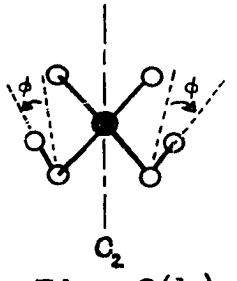

Fig. 2(b)

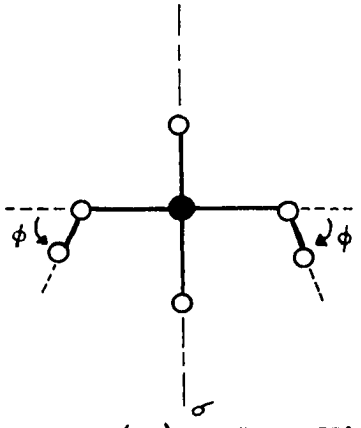

Fig. 3(a).--Top View

C_s

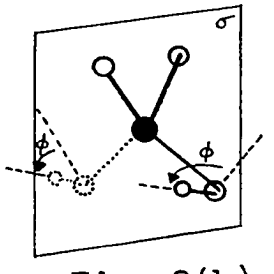

Fig. 3(b)

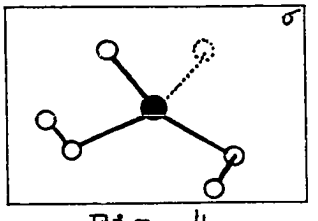

Fig. 4

Legend

● Lead

○ Carbon

TABLE XIV

CLASSIFICATION OF THE SIXTY-THREE NORMAL VIBRATIONS OF DMDEL FOR DIFFERENT MOLECULAR SYMMETRIES[a]

Approximate Character	C_{2v}				C_2		$C_s(a)$		$C_s(b)$	
	$*a_1^+$	$*a_2$	$*b_1^+$	$*b_2^+$	$*a^+$	$*b^+$	$*a'^+ + *a''^+$		$*a'^+ + *a''^+$	
Methyl										
$(CH_3)'$ asym. str.	1	1	1	1	2	2	2	2	2	2
CH_3 asym. str.	1	1	1	1	2	2	2	2	2	2
$(CH_3)'$ sym. str.	1	0	1	0	1	1	1	1	2	0
CH_3 sym. str.	1	0	0	1	1	1	2	0	1	1
$(CH_3)'$ asym. def.	1	1	1	1	2	2	2	2	2	2
CH_3 asym. def.	1	1	1	1	2	2	2	2	2	2
$(CH_3)'$ sym. def.	1	0	1	0	1	1	1	1	2	0
CH_3 sym. def.	1	0	0	1	1	1	2	0	1	1
$(CH_3)'$ rocking	1	1	1	1	2	2	2	2	2	2
CH_3 rocking	1	1	1	1	2	2	2	2	2	2
$(CH_3)'$ torsion	0	1	0	1	1	1	1	1	0	2
CH_3 torsion	0	1	1	0	1	1	0	2	1	1
Methylene										
CH_2 asym. str.	0	1	0	1	1	1	1	1	0	2
CH_2 sym. str.	1	0	1	0	1	1	1	1	2	0
CH_2 def. (bending)	1	0	1	0	1	1	1	1	2	0
CH_2 wagging	1	0	1	0	1	1	1	1	2	0
CH_2 twisting	0	1	0	1	1	1	1	1	0	2
CH_2 rocking	0	1	0	1	1	1	1	1	0	2
Skeletal										
C-C stretching	1	0	1	0	1	1	1	1	2	0
Pb-C stretching	1	0	0	1	1	1	2	0	1	1
$(Pb-C)'$ stretching	1	0	1	0	1	1	1	1	2	0
Pb-C-C bending	1	0	1	0	1	1	1	1	2	0
Pb-C-C twisting	0	1	0	1	1	1	1	1	0	2
C-Pb-C def.	2	1	1	1	3	2	3	2	3	2
Total	19	13	16	15	32	31	34	29	35	28

[a] $(CH_3)'$ = methyl group not bonded directly to lead atom; $(Pb-C)'$ = lead-carbon bond between lead atom and methylene group; * = Raman active; + = infrared active.

Possible Symmetry of MTEL

The lead-carbon skeleton can, at most, have the symmetry C_{3v}. Two configurations with this symmetry are possible. These are shown in Plate III, Figs. 1(a) and 1(b), page 78.

If the three ethyl groups are rotated from the positions shown in Plate III, Fig. 1(a) or 1(b) through an angle $\phi(\neq 0^{\circ}, \neq 180^{\circ})$ in the same sense (see Plate III, Fig. 2) the molecule will have the symmetry C_3. There are an infinite number of these configurations since ϕ is arbitrary.

If one of the ethyl groups is not rotated, and the other two are rotated through equal but opposite angles $\phi(\neq 0^{\circ})$, the molecule will have the symmetry C_s, with the two rotated ethyl groups forming mirror images of each other upon reflection in the symmetry plane. There will be an infinite number of these possible configurations, one of which is shown in Plate III, Fig. 3(a).

If one of the ethyl groups is rotated through 180°, and the other two through equal but opposite angles $\phi(\neq 180^{\circ})$, the molecule will again have the symmetry C_s. There will be an infinite number of possible configurations of this type since ϕ is arbitrary. One of these is shown in Plate III, Fig. 3(b).

The distribution of the 72 normal vibrations for these different possible molecular symmetries is given in Table XV, page 79.

PLATE III

POSSIBLE CONFIGURATIONS OF
LEAD-CARBON SKELETON IN MTEL

C_{3v}

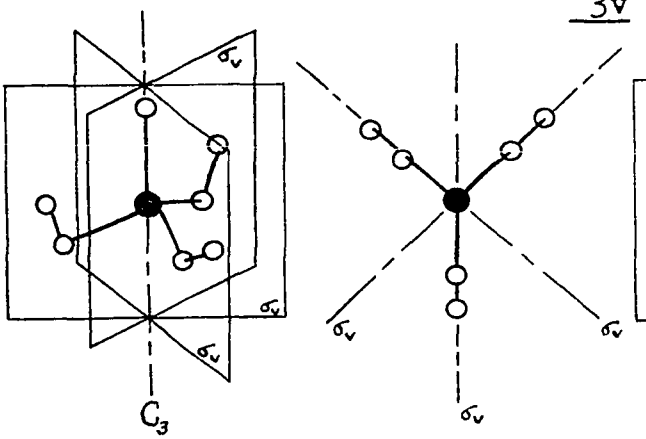

Fig. 1(a)

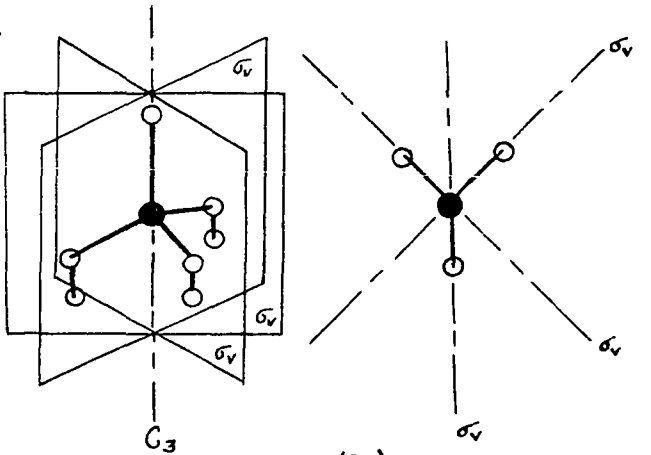

Fig. 1(b)

C_3



Fig. 2

C_s

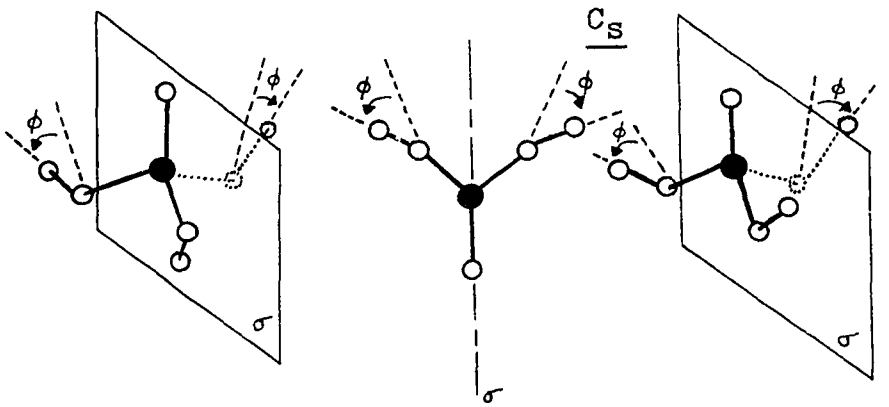

Fig. 3(a)

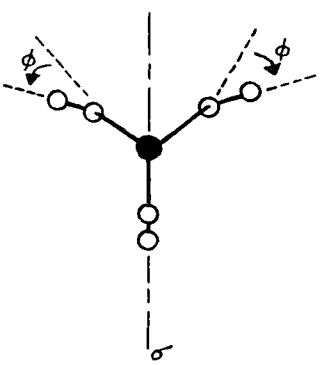

Fig. 3(b)

Legend

● Lead
○ Carbon

TABLE XV

CLASSIFICATION OF THE SEVENTY-TWO NORMAL VIBRATIONS OF MTEL FOR DIFFERENT MOLECULAR SYMMETRIES[a]

Approximate Character	C_{3v}			C_3		C_s	
	$*a_1^+$	a_2	$*e^+$	$*a^+$	$*e^+$	$*a'^+$	$*a''^+$
Methyl							
$(CH_3)'$ asym. str.	1	1	2	2	2	3	3
CH_3 asym. str.	0	0	1	0	1	1	1
$(CH_3)'$ sym. str.	1	0	1	1	1	2	1
CH_3 sym. str.	1	0	0	1	0	1	0
$(CH_3)'$ asym. def.	1	1	2	2	2	3	3
CH_3 asym. def.	0	0	1	0	1	1	1
$(CH_3)'$ sym. def.	1	0	1	1	1	2	1
CH_3 sym. def.	1	0	0	1	0	1	0
$(CH_3)'$ rocking	1	1	2	2	2	3	3
CH_3 rocking	0	0	1	0	1	1	1
$(CH_3)'$ torsion	0	1	1	1	1	1	2
CH_3 torsion	0	1	0	1	0	0	1
Methylene							
CH_2 asym. str.	0	1	1	1	1	1	2
CH_2 sym. str.	1	0	1	1	1	2	1
CH_2 def.	1	0	1	1	1	2	1
CH_2 wagging	1	0	1	1	1	2	1
CH_2 twisting	0	1	1	1	1	1	2
CH_2 rocking	0	1	1	1	1	1	2
Skeletal							
C-C stretching	1	0	1	1	1	2	1
Pb-C stretching	1	0	0	1	0	1	0
$(Pb-C)'$ stretching	1	0	1	1	1	2	1
Pb-C-C bending	1	0	1	1	1	2	1
Pb-C-C twisting	0	1	1	1	1	1	2
C-Pb-C def.	1	0	2	1	2	3	2
Total	15	9	24	24	24	39	33

[a] $(CH_3)'$ = methyl group not bonded directly to lead atom; $(Pb-C)'$ = lead-carbon bond between lead atom and methylene group; * = Raman active; + = infrared active.

Possible Symmetry of TEL

The lead-carbon skeleton can, at most, have the symmetry D_{2d}. The two possible configurations with this symmetry are shown in Plate IV, Figs. 1(a) and 1(b), pages 82 through 84.

If the ethyl groups are rotated about the lead-carbon bonds through an angle $\phi(\neq 0^\circ, \neq 180^\circ)$ from their position in Plate IV, Figs. 1(a) or 1(b), the other two through the same angle, but opposite in sense, as shown in Plate IV, Fig. 4, page 84, the molecule will have the symmetry D_2. There will be an infinite number of these possible configurations since there are an infinite number of possible values for ϕ.

If two of the ethyl groups are rotated about the lead-carbon bonds in a positive sense, when viewed along the bond, and the other two are rotated through the same angle but in a negative sense, as shown in Plate IV, Fig. 5, page 84, the molecule will have the symmetry S_4. There will again be an infinite number of these possible configurations.

If two of the ethyl groups are rotated through 180° and the other two left unchanged, the molecule has the symmetry C_{2v}. This is the only possible configuration with this symmetry, and is shown in Plate IV, Fig. 2, page 83.

If two of the ethyl groups are rotated through an angle $\phi_1(\neq 0^\circ, \neq 180^\circ)$ in the same sense, and the other ethyl groups are rotated through a different angle $\phi_2(= 0^\circ, = 180^\circ)$,

as shown in Plate IV, Fig. 3, page 83, the molecule will have the symmetry C_2. Since both ϕ_1, and ϕ_2 are arbitrary and independent of each other, there will be a doubly infinite set of possible configurations with this symmetry.

If one of the ethyl groups is rotated through 180° and two others rotated through an arbitrary angle so that they are mirror images of each other when reflected in the plane of symmetry, as shown in Plate IV, Fig. 6, page 84, the molecule has the symmetry C_s. There are an infinite number of these possible configurations.

The distributions of the 81 normal vibrations among symmetry species in the different cases are given in Table XVI, page 85.

PLATE IV

POSSIBLE CONFIGURATIONS OF
LEAD-CARBON SKELETON IN TEL

$\underline{D_{2d} \equiv V_d}$

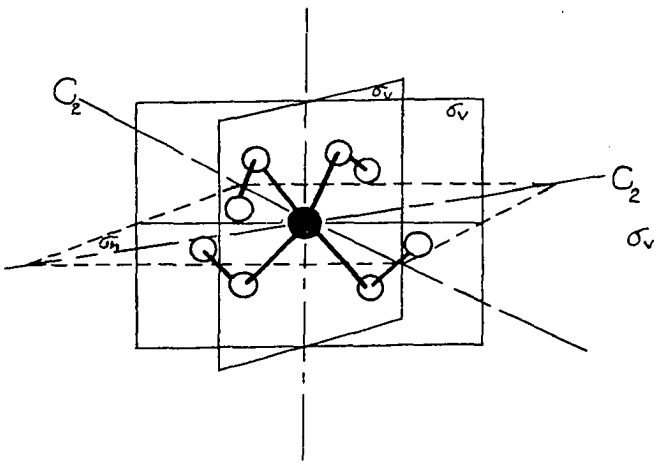

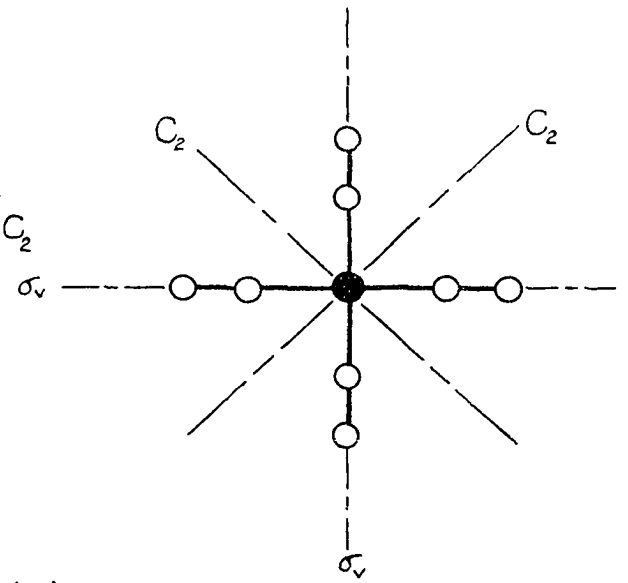

Fig. 1(a) Top View

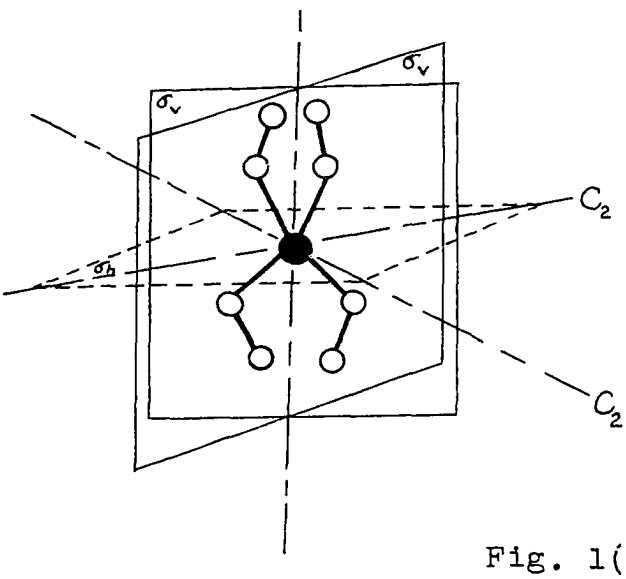

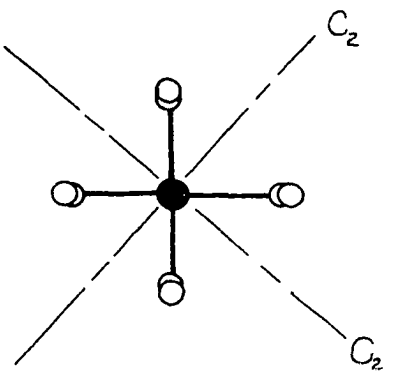

Fig. 1(b)

Legend

● Lead

○ Carbon

PLATE IV --Continued

C_{2v}

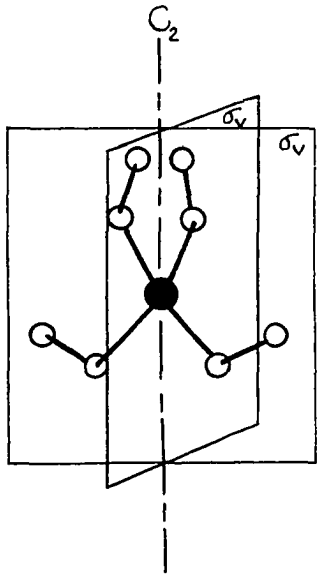

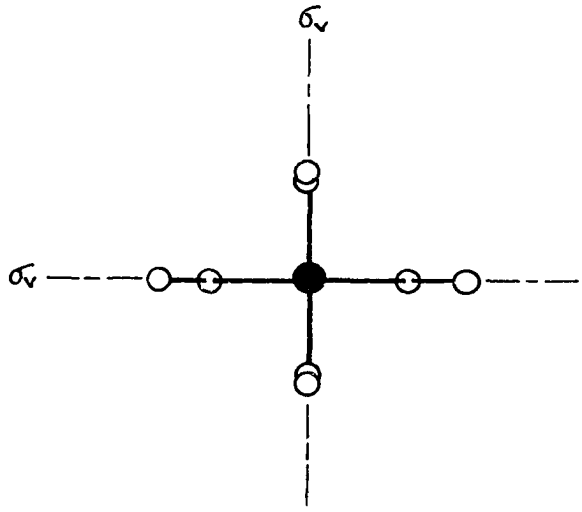

Fig. 2 Top View

C_2

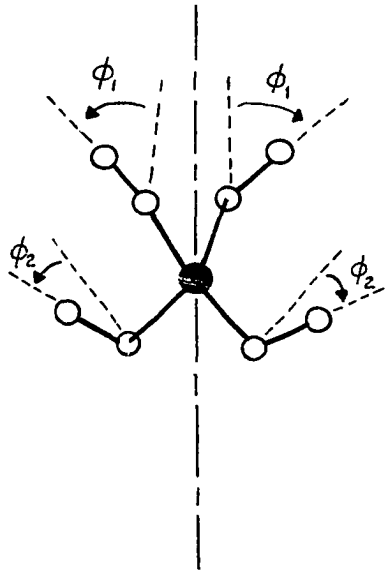

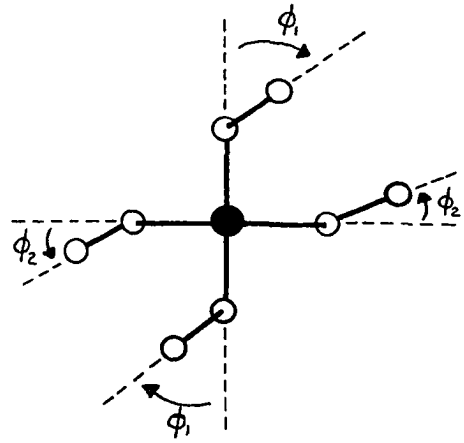

Top View

Fig. 3

PLATE IV--Continued

D_2

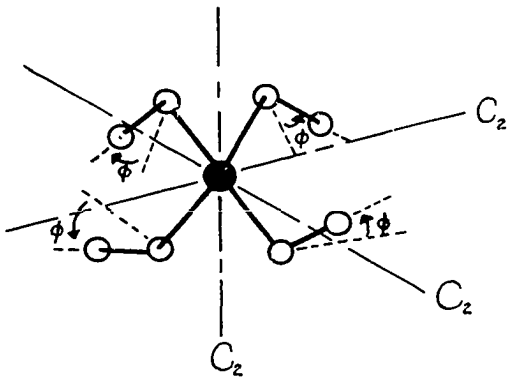

Fig. 4

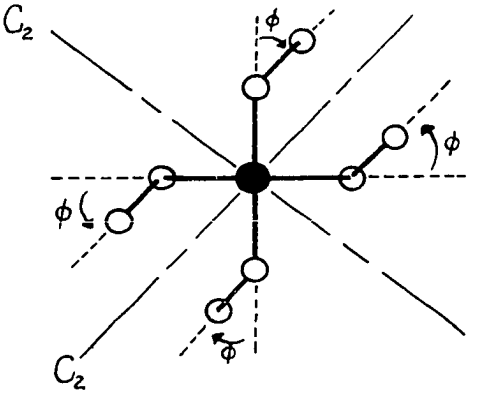

Top View

S_4

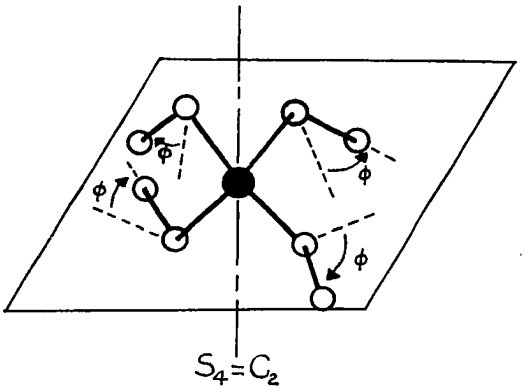

Fig. 5

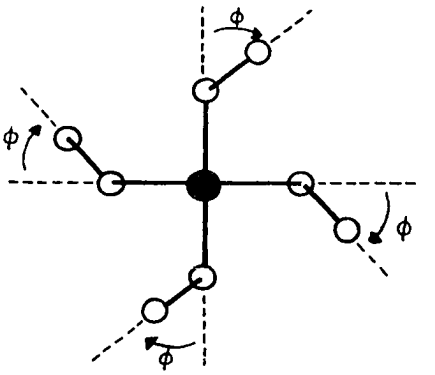

Top View

C_s

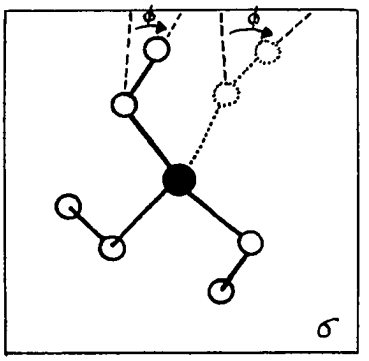

Fig. 6

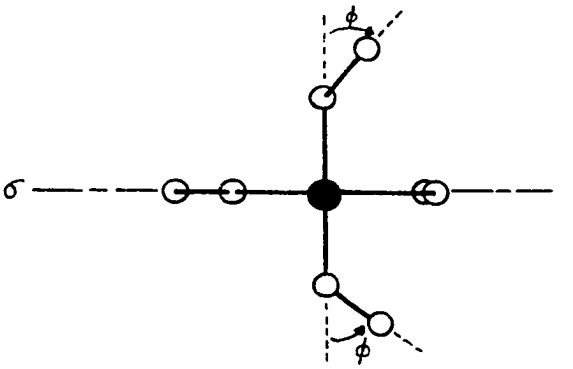

Top View

TABLE XVI

CLASSIFICATION OF THE EIGHTY-ONE NORMAL VIBRATIONS OF TEL FOR DIFFERENT MOLECULAR SYMMETRIES

Approximate Character	$D_{2d} \equiv V_d$					C_{2v}				C_2		$D_2 \equiv V$				S_4			C_s	
	$^*a_1$	a_2	$^*b_1$	$^*b_2^+$	$^*e^+$	$^*a_1^+$	$^*a_2$	$^*b_1^+$	$^*b_2^+$	$^*a^+$	$^*b^+$	$^*a$	$^*b_1^+$	$^*b_2^+$	$^*b_3^+$	$^*a^+$	$^*b$	$^*e^+$	$^*a'^+$	$^*a''^+$
Methyl																				
$(CH_3)'$ asym. str.	1	1	1	1	2	2	2	2	2	4	4	2	2	2	2	2	2	2	4	4
$(CH_3)'$ sym. str.	1	0	0	1	1	2	0	1	1	2	2	1	1	1	1	1	1	1	3	1
$(CH_3)'$ asym. def.	1	1	1	1	2	2	2	2	2	4	4	2	2	2	2	2	2	2	4	4
$(CH_3)'$ sym. def.	1	0	0	1	1	2	0	1	1	2	2	1	1	1	1	1	1	1	3	1
$(CH_3)'$ rocking	1	1	1	1	2	2	2	2	2	4	4	2	2	2	2	2	2	2	4	4
$(CH_3)'$ torsion	0	1	1	0	1	2	0	1	1	2	2	1	1	1	1	1	1	1	1	3
Methylene																				
CH_2 asym. str.	0	1	1	0	1	0	2	1	1	2	2	1	1	1	1	1	1	1	1	3
CH_2 sym. str.	1	0	0	1	1	2	0	1	1	2	2	1	1	1	1	1	1	1	3	1
CH_2 def.	1	0	0	1	1	2	0	1	1	2	2	1	1	1	1	1	1	1	3	1
CH_2 wagging	1	0	0	1	1	2	0	1	1	2	2	1	1	1	1	1	1	1	3	1
CH_2 twisting	0	1	1	0	1	0	2	1	1	2	2	1	1	1	1	1	1	1	1	3
CH_2 rocking	0	1	1	0	1	0	2	1	1	2	2	1	1	1	1	1	1	1	1	3
Skeletal																				
C-C stretching	1	0	0	1	1	2	0	1	1	2	2	1	1	1	1	1	1	1	3	1
$(Pb-C)'$ str.	1	0	0	1	1	2	0	1	1	2	2	1	1	1	1	1	1	1	3	1
Pb-C-C bending	1	0	0	1	1	2	0	1	1	2	2	1	1	1	1	1	1	1	3	1
Pb-C-C twisting	0	1	1	0	1	0	2	1	1	2	2	1	1	1	1	1	1	1	1	3
C-Pb-C def.	1	0	1	1	1	2	1	1	1	3	2	2	1	1	1	1	2	1	3	2
Total	12	8	9	12	20	24	17	20	20	41	40	21	20	20	20	20	21	20	44	37

CHAPTER VI

INTERPRETATION OF THE VIBRATIONAL SPECTRA OF TML

The assignment of Young, Koehler, and McKinney (19) was extended and modified by Pitzer and Sheline (17), Lippincott and Tobin (14), and by Hall (7). The assignment adopted here is essentially the same as Hall's, with the exception of the interchange of $\nu_8(e)$ and $\nu_{14}(f_2)$, and a slight change in the assignment of $\nu_7(e)$.

The symmetry of the PbC_4 skeleton is believed to be T_d. With proper orientation of the methyl groups, the molecule as a whole will also have this symmetry. The lack of infrared activity of the symmetric methyl deformation band at 1169 cm^{-1} lends support to the belief that the molecule has this symmetry. For definiteness and convenience this will be assumed, and the numbering of fundamentals of Young, et al., will be used.

According to Table XVII, page 87, there should be four observable Raman and two infrared fundamental bands, involving largely C-H stretching and lying in the 2900-3000 cm^{-1} region. Of these, one a_1 and one f_2 vibration should involve symmetrical, and one e and one f_2 asymmetrical stretching of

TABLE XVII

DISTRIBUTION OF FUNDAMENTAL VIBRATIONS FOR TML OF SYMMETRY T_d [a]

Approximate Character	Symmetry Species				
	*a_1	a_2	*e	f_1	*f_2+
CH_3 asym. stretching			ν_5(2998)	ν_9(~3000)	ν_{13}(2998)
CH_3 sym. stretching	ν_1(2918)				ν_{14}(2918)
CH_3 asym. def.			ν_6(1412)	ν_{10}(~1450)	ν_{15}(1455)
CH_3 sym. def.	ν_2(1169)				ν_{16}(1157)
CH_3 rocking			ν_7(~800)	ν_{11}(750-800?)	ν_{17}(769)
Pb-C stretching	ν_3(462)				ν_{18}(475)
Skeletal def.			ν_8(145)		ν_{19}(130)
CH_3 torsion		ν_4(~215)		ν_{12}(~215)	

[a] * = Raman active; + = infrared active; the wave numbers given in parentheses are those assigned in the present work.

the methyl groups. The two f_2 vibrations should be infrared active. Raman bands are found at 2918 cm^{-1} and 2998 cm^{-1}, the band at 2918 cm^{-1} being polarized. Infrared bands were observed by all workers at approximately these frequencies, the experimental error being rather large due to low resolution in this region.

The Raman bands are rather diffuse, as would be expected if each is the superposition of two adjacent bands. Since f_2 is the only species active in the infrared, the two asymmetrical CH_3 stretching vibrations $\nu_5(e)$ and $\nu_{13}(f_2)$ are assigned to the bands at 2998 cm^{-1}, and the two symmetrical CH_3 stretching vibrations $\nu_1(a_1)$ and $\nu_{14}(f_2)$ are assigned to the bands at 2918 cm^{-1}.

Two weak, diffuse Raman bands are observed at 1412 cm^{-1} and 1455 cm^{-1}. Strong infrared bands are observed at 1412 cm^{-1} and 1452 cm^{-1} in the liquid, in essential agreement with previous investigators.

The vibrations expected to be in this frequency range are those involving asymmetric CH_3 deformation, i.e. $\nu_6(e)$, $\nu_{10}(f_1)$, and $\nu_{15}(f_2)$. In agreement with the assignments of previous workers, the band at 1455 cm^{-1} is taken to be the triply degenerate fundamental $\nu_{15}(f_2)$. This is consistent with its being both infrared and Raman active. The fundamental $\nu_{10}(f_1)$ should be inactive in both Raman and infrared spectra. The fundamental $\nu_6(e)$ is believed by Pitzer and Sheline to be also at 1455 cm^{-1}, while it is identified

by Hall with the band at 1412 cm^{-1}, and by Lippincott and Tobin with what is evidently the same band observed by them at 1400 cm^{-1}. Pitzer and Sheline reported a band at 1392 cm^{-1} in the infrared spectrum and interpreted it as the ternary combinations $2\nu_3(a_1) + \nu_{18}(f_2)$.

There are no binary combinations of observed fundamentals that would account for the band at 1412 cm^{-1}, and it seems doubtful that it could result from a binary combination involving one of the inactive fundamentals, since the inactive methyl rocking fundamental $\nu_{11}(f_1)$ presumably lies in the range 750-800 cm^{-1}, near $\nu_7(e)$ and $\nu_{17}(f_2)$, and since the present assignment shows that the two inactive torsional modes $\nu_4(a_2)$ and $\nu_{12}(f_1)$ probably have values near 215 cm^{-1}. It could be explained as the ternary combination $2\nu_{18} + \nu_3$, but this does not seem plausible since ternary combinations rarely occur in Raman spectra with the observed intensity. The band at 1412 cm^{-1} is therefore interpreted as the doubly degenerate vibration $\nu_6(e)$. Its activity in the infrared may be a result of breakdown of the selection rules in the liquid state, or of Coriolis coupling between one or more of the pairs of vibrations $\nu_6(e)$ and $\nu_{15}(f_2)$, $\nu_6(e)$ and $\nu_{10}(f_1)$, and $\nu_{10}(f_1)$ and $\nu_{15}(f_2)$, even though the rotation in the liquid state may not be completely free. The diffuse nature of these bands indicates that Coriolis interaction actually occurs.

In the 1100-1200 cm^{-1} region there are two very strong, sharp Raman bands at 1157 cm^{-1} and 1169 cm^{-1}, the latter

being polarized. A strong, sharp infrared band is observed at 1152 cm^{-1} and a weak shoulder at 1165 cm^{-1}.

In agreement with previous assignments, these bands are ascribed to vibrations consisting largely of symmetrical deformation of the methyl groups. The polarized Raman band at 1169 cm^{-1} is identified with $\nu_2(a_1)$ and the band at 1157 cm^{-1} with $\nu_{16}(f_2)$. The weak infrared band at 1165 cm^{-1} may result from breakdown of the selection rules in the liquid state.

There should be three vibrations $\nu_7(e)$, $\nu_{11}(f_1)$, and $\nu_{17}(f_2)$ consisting largely of rocking of the methyl groups. Pitzer and Sheline, and Hall, assign both $\nu_7(e)$ and $\nu_{17}(f_2)$ to the diffuse Raman band at 769 cm^{-1}, while Lippincott and Tobin interpreted this band as $\nu_{17}(f_2)$ and assigned $\nu_7(e)$ to a weak band which they observed in the Raman spectrum at 700 cm^{-1}. They assume that the inactive $\nu_{11}(f_1)$ has the same frequency as $\nu_{17}(f_2)$.

A careful study of the Raman band at 769 cm^{-1} shows it to be slightly asymmetric, with a shoulder extending from the peak at 769 cm^{-1} toward higher frequencies. This band is therefore believed to be the superposition of a band at 769 cm^{-1} and a much weaker band at approximately 800 cm^{-1}. Its resolution is shown on a logarithmic scale in Fig. 18, page 91.

The infrared spectrum of the vapor obtained by Swanson shows a band with PQR structure at 769 cm^{-1} and, in addition,

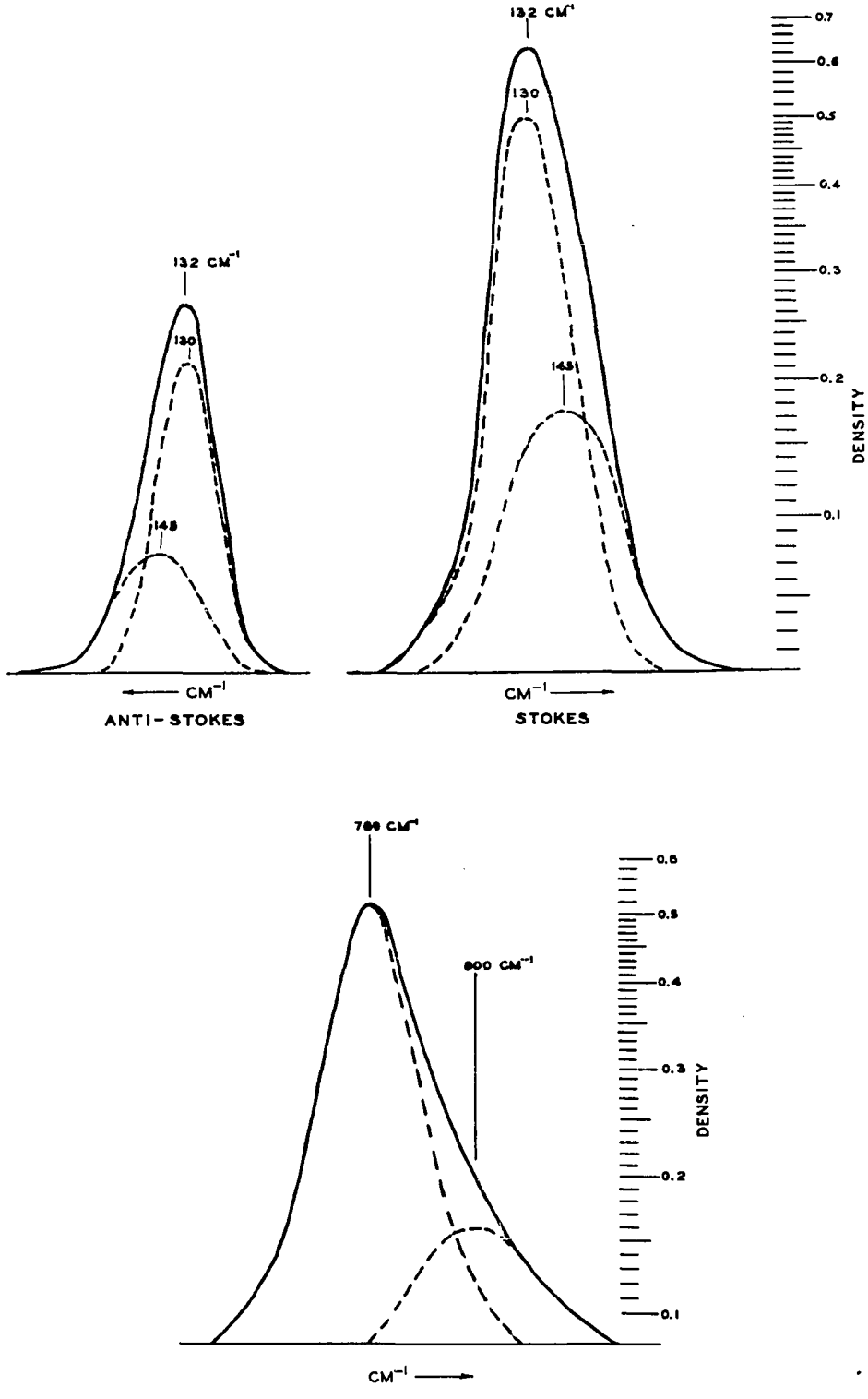

Fig. 18. Resolution of Raman Bands in TML

a definite shoulder at 796 cm^{-1}, while Pitzer and Sheline observe only the PQR structure at 769 cm^{-1}. Since Swanson used an instrument of somewhat higher resolution than that of Pitzer and Sheline, her observation is taken as a confirmation of the presence of two Raman bands.

The band at 769 cm^{-1} is interpreted as the f_2 fundamental ν_{17}, and the band near 800 cm^{-1} as $\nu_7(e)$. The activity of $\nu_7(e)$ in the infrared may be the result of selection rule breakdown in the liquid, or of Coriolis interaction between $\nu_7(e)$, $\nu_{11}(f_1)$, and $\nu_{17}(f_2)$.

The four fundamental vibrations of the lead-carbon skeleton $\nu_3(a_1)$, $\nu_8(e)$, $\nu_{18}(f_2)$, and $\nu_{19}(f_2)$ should resemble the vibrations of XY_4 molecules, although they may, of course, be more or less mixed with methyl vibrations. The a_1 "breathing" vibration and the doubly degenerate vibration are uniquely determined. They are shown in Figs. 19(a) and 19(b), page 93. However, since there are two vibrations of species f_2, their actual forms are not determined by symmetry alone. Herzberg (9) gives possible forms for these vibrations. Another set of possible normal vibrations of an XY_4 molecule is shown in Figs. 19(c) and 19(d), page 93. The vibration in Fig. 19(c) can be described approximately as an asymmetrical stretching of the X-Y bonds in which two bonds stretch out of phase with the other two. The other vibration of species f_2, Fig. 19(d) , which must be orthogonal to the vibration in Fig. 19(c), is a vibration in which the Y atoms

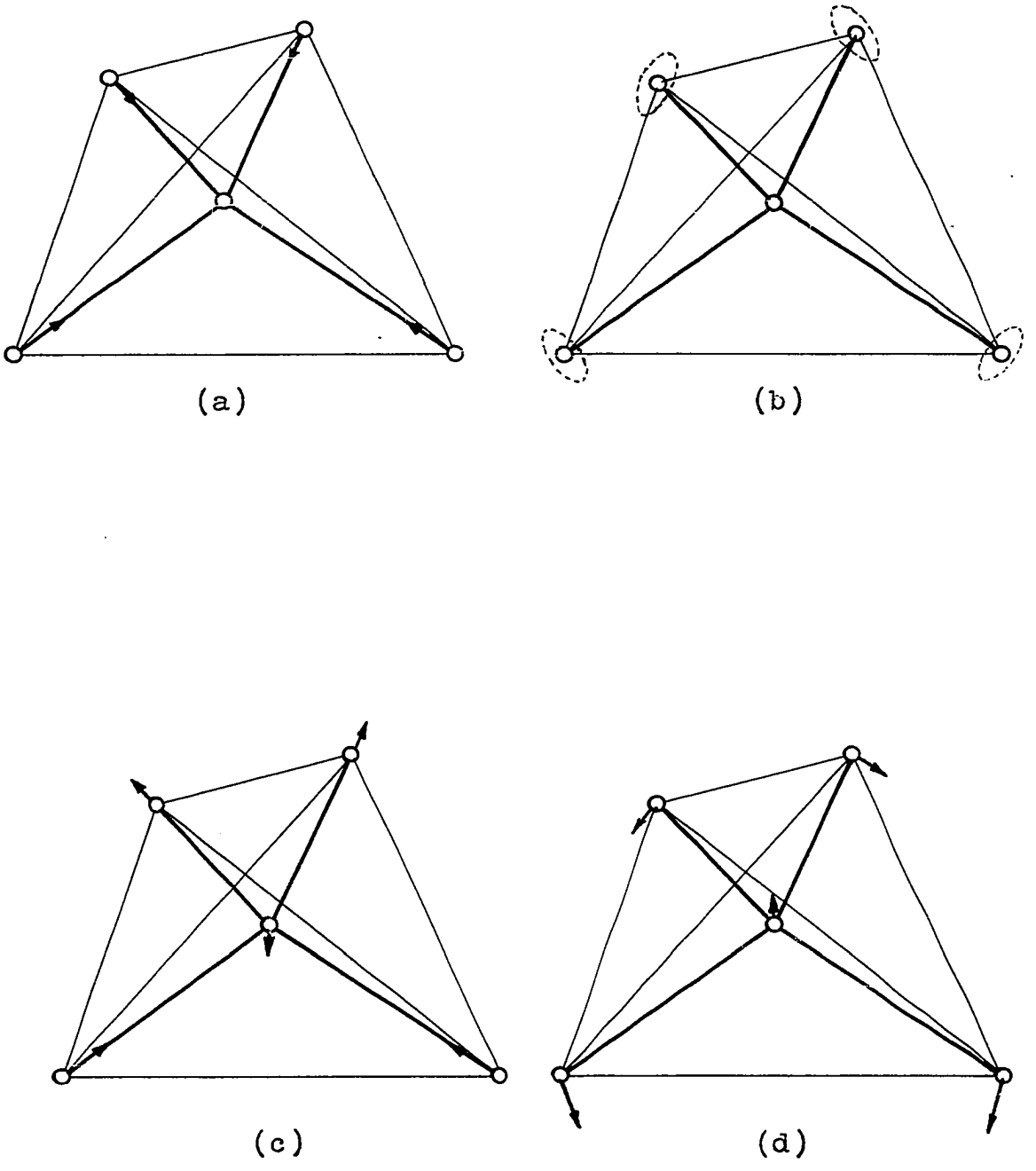

Fig. 19. Normal Vibrations of XY_4 Molecule

move essentially perpendicular to the X-Y bonds.

The very strong, sharp, polarized Raman band at 462 cm^{-1} is interpreted as $\nu_3(a_1)$, while the strong band observed at 475 cm^{-1} in the Raman spectrum, and at 476 cm^{-1} in the infrared by Pitzer and Sheline, is interpreted as $\nu_{18}(f_2)$. Although it seems peculiar that these two fundamentals should be so close together, this is consistent with the assignments made for other molecules of the $A(CH_3)_4$ type, as shown by the correlation diagram in Fig. 20, page 95. The close proximity of $\nu_{18}(f_2)$ at 475 cm^{-1} to $\nu_3(a_1)$ at 462 cm^{-1} means that $\nu_{18}(f_2)$ must be largely Pb-C stretching, as shown in Fig. 19(c), page 93.

The strong, diffuse Raman band at 132 cm^{-1} is believed to be the superposition of $\nu_8(e)$ and $\nu_{19}(f_2)$, since it is asymmetric, having a shoulder extending toward higher frequencies from the peak at ~132 cm^{-1}. The resolution of a microphotometer trace of this band into its components at ~130 cm^{-1} and ~145 cm^{-1} is shown on a logarithmic scale in Fig. 18, page 91. The peak frequencies could not be changed very much without distorting the shape of the bands into unreasonable contours. The resolution shown is therefore believed to be essentially correct.

The fundamental $\nu_8(e)$ is taken to be 145 cm^{-1} and $\nu_{19}(f_2)$ to be 130 cm^{-1}. This assignment of $\nu_8(e)$ to a higher frequency than ν_{19} disagrees with the interpretation of Lippincott and Tobin (14), and Hall (7). It is in

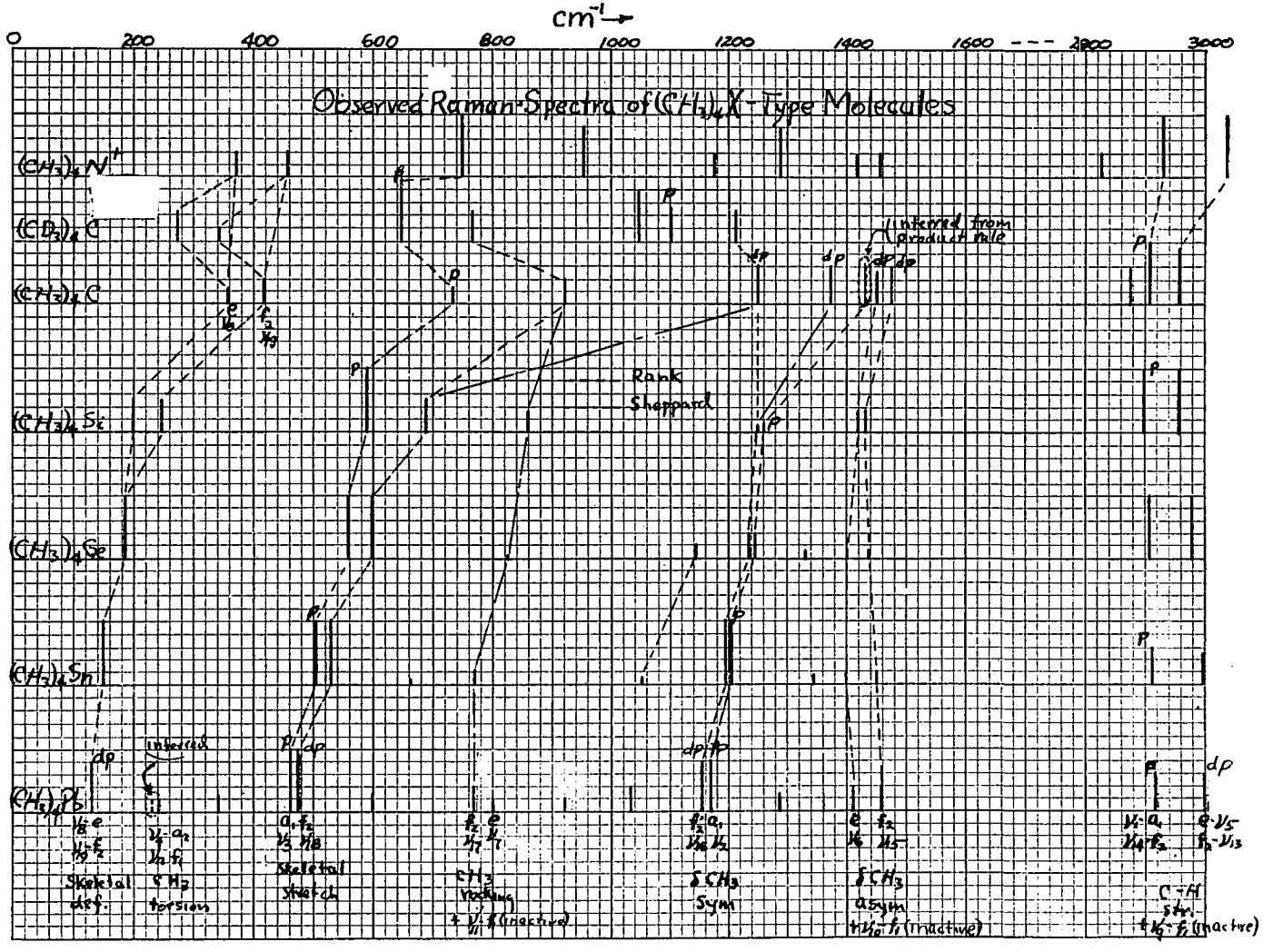

Fig. 20. Observed Raman Spectra of $(CH_3)_4$ X-Type Molecules

agreement, however, with the diagram for XY_4-type molecules given by Kohlrausch (12) if the methyl groups in TML are considered to be point masses. The requirement that the form of $\nu_{18}(f_2)$ be as shown in Fig. 19(c), page 93, means that $\nu_{19}(f_2)$ is of the form shown in Fig. 19(d), since these two motions must be orthogonal to each other. The doubly degenerate fundamental $\nu_8(e)$ corresponds to a motion of the XY_4 molecule in which the Y atoms move perpendicular to the X-Y bonds. The close proximity of ν_8 and ν_{19}, then lends support to the association of ν_{19} with the form shown in Fig. 19(d). In this motion the Y atoms move essentially perpendicular to the X-Y bonds, since the large $Pb/(CH_3)$ mass ratio means that the lead atom moves very little (the amplitude of this motion in Fig. 19 is exaggerated).

The two vibrations $\nu_4(a_2)$ and $\nu_{12}(f_1)$, consisting largely of torsional oscillations of the methyl groups about the lead-carbon bonds, are not active in either the Raman or infrared spectrum. However, they may form active combination bands.

A weak, diffuse Raman band is observed at 342 cm^{-1}, both as a Stokes and an anti-Stokes band. It was interpreted by Hall as a C-H stretching fundamental excited by the mercury line at 3919 A^o. That this is not correct is shown by the fact that, in the present work, the exciting lines of wavelength shorter than 4300 A^o were prevented from reaching the sample. The band cannot be due to an impurity, since only

a few of the possible impurities have a band near this frequency, and all of these have stronger bands that are not observed. It could be interpreted as the difference band $\nu_{18}(f_2) - \nu_{19}(f_2)$, 475 - 130 = 345($A_1$+E+$F_1$+$F_2$), which would require that the band at 598 cm^{-1} be interpreted as the sum band $\nu_{18} + \nu_{19}$, 475 + 130 = 605. However, this is not plausible, since observable difference bands are rare, especially as anti-Stokes bands.

This band is therefore interpreted as one or more of the combinations $\nu_8(e) + \nu_4(a_2)$, $\nu_8(e) + \nu_{12}(f_1)$, and $\nu_{19}(f_2) + \nu_{12}(f_1)$. The first two of these combinations would give a value of 197 cm^{-1} for either ν_4 and ν_{12}, or both, while the last would place ν_{12} at 212 cm^{-1}.

A further indication of the value of the torsional frequencies is obtained from the interpretation of the broad, weak Raman band at 692 cm^{-1}. This band cannot be explained as a combination of ν_8, ν_{19}, ν_3, or ν_{18}, and none of the likely impurities have a band at this frequency. If the band is interpreted as the combination $\nu_{12}(f_1) + \nu_{18}(f_2)$($A_2$+E+$F_1$ +F_2), ν_{12} comes out to be 217 cm^{-1}, in fair agreement with the value 212 cm^{-1}.

Other Raman bands which cannot be explained as binary combinations of observed fundamentals are the very weak, sharp band at 1004 cm^{-1} and the weak, diffuse band at 1033 cm^{-1}. Pitzer and Sheline observed infrared bands at 1022 cm^{-1} and 1051 cm^{-1} which they interpreted as the difference bands

$\nu_{16}(f_2) - \nu_{19}(f_2)$, and $\nu_{16}(f_2) - \nu_8(e)$, respectively. Neither of these interpretations is believed to be adequate, since Pitzer and Sheline's assignments of ν_8 and ν_{19} were adjusted to agree with a Raman band at 577 cm^{-1} reported by Duncan and Murray (5). In the present work, a Raman band was found at 598 cm^{-1} but none at 577 cm^{-1}.

The Raman band observed a 1033 cm^{-1} in the present work may be interpreted as the difference band $\nu_{16} - \nu_{19}$ (1157 - 130 = 1025 cm^{-1}) corresponding to the sum band at 1286 cm^{-1}. It can also be interpreted as a binary combination of one of the inactive torsional fundamentals $\nu_4(a_2), \nu_{12}(f_1)$ and one of the methyl rocking fundamentals $\nu_7(e)$, $\nu_{11}(f_1)$. A binary combination of the torsional and rocking modes could also account for the weak, sharp Raman band at 1004 cm^{-1} which cannot be explained as a binary combination of observed fundamentals.

The other observed bands are interpreted as binary combinations as reported in Table II, page 42.

Discussion of the Raman Spectrum of Crystalline TML

In the 3000 cm^{-1} region, where the bands associated with C-H stretching occur, no significant difference is found between the spectra of liquid and crystalline TML.

In the region of the bands involving symmetrical methyl deformation one very intense and sharp band at 1157 and two weak, sharp bands at 1150 and 1141 cm^{-1} are found

in crystalline TML, as compared to the two very strong bands in the liquid at 1169 and 1157 cm^{-1}, interpreted as a_1, and f_2 fundamentals, respectively. What appears to happen as the phase changes from liquid to crystal is that the a_1 fundamental shifts from 1169 to 1157 cm^{-1}, while the f_2 fundamental at 1157 cm^{-1} is shifted and split into two components. This interpretation is somewhat weakened by the curious fact that the shifted position of the a_1 fundamental coincides with the unshifted position of the f_2 fundamental.

Like most of the other bands, the very strong a_1 fundamental at 462 cm^{-1}, associated with a breathing vibration of the molecular skeleton, is much sharper in the crystal than in the liquid, but it is shifted very little, occurring at 463 cm^{-1}. The strong f_2 fundamental at 475 cm^{-1}, on the other hand, is split into two components at 474 and 471 cm^{-1}.

In the region where the two lowest skeletal frequencies occur, there is considerable background. However, it appears that the fundamental bands at 145 and 130 cm^{-1} in the liquid shift to 170 and 155 cm^{-1} in the crystalline state.

The structure of crystalline TML is not known. However, if it is assumed that the molecular site group is T_d, T_h, or T, the theory of Hornig (9) shows that there should be no splitting of the doubly degenerate fundamentals, while a splitting of the triply degenerate fundamentals may occur as a result of interaction with a triply degenerate lattice vibration t(F) or R(F) if the site group is T, $T(F_2)$ if it

is T_d, and $R(F_g)$ if it is T_h. The observed splitting of the two f_2 fundamentals is in general accord with this prediction.

The great sharpness of most of the Raman bands of crystalline TML, while partly a result of the low temperature ($-70^{\circ}C$) at which the observations were made, shows that the harmonic oscillator approximation is good for most of the fundamental vibrations of TML (9).

CHAPTER VII

INTERPRETATION OF THE SPECTRA OF TMEL, DMDEL, MTEL, AND TEL

Since each of these molecules probably exists in several different configurations, as indicated in Chapter V, a detailed interpretation, such as was given for TML, is not feasible.

Because of the large number of fundamentals for these molecules, the interpretation is complicated by the fact that Fermi resonance is possible in several frequency regions.

The fact that certain infrared and Raman bands are found at nearly the same frequency and relative intensity in all the lead alkyls suggests that a discussion of the spectra in terms of "group" frequencies might be useful.

The numbers of Raman and infrared active fundamentals expected in each region for different molecular symmetries are given in Tables XVIII, page 102, and XIX, page 104, respectively. Since some bands will overlap, the number of resolved bands will usually be smaller.

The best Raman and infrared data for the lead alkyls series are correlated graphically in Fig. 21, page 107, for

TABLE XVIII

NUMBER OF RAMAN ACTIVE FUNDAMENTALS EXPECTED IN DIFFERENT FREQUENCY REGIONS FOR DIFFERENT MOLECULAR SYMMETRIES[a]

Region and Characteristic Vibration	Molecular Symmetry												
	TMEL	DMDEL			MTEL			TEL					
	C_s	C_{2v}	C_2	C_s	C_{3v}	C_3	C_s	D_{2d}	C_{2v}	C_2	D_2	S_4	C_s
2800-3000 cm^{-1}													
$(CH_3)'$ asym. str.	2	4	4	4	3	4	6	5	8	8	8	6	8
CH_3 asym. str.	6	4	4	4	1	1	2	0	0	0	0	0	0
CH_2 asym. str.	1	2	2	2	1	2	3	2	4	4	4	3	4
$(CH_3)'$ sym. str.	1	2	2	2	2	2	3	3	4	4	4	3	4
CH_3 sym. str.	3	2	2	2	1	1	1	0	0	0	0	0	0
CH_2 sym. str.	1	2	2	2	2	2	3	3	4	4	4	3	4
Total	14	16	16	16	10	12	18	13	20	20	20	15	20
1100-1500 cm^{-1}													
$(CH_3)'$ asym. def.	2	4	4	4	3	4	6	5	8	8	8	6	8
CH_3 asym. def.	6	4	4	4	1	1	2	0	4	0	0	0	0
CH_2 def.	1	2	2	2	2	2	3	3	4	4	4	3	4
CH_2 wagging	1	2	2	2	2	2	3	3	4	4	4	3	4
$(CH_3)'$ sym. def.	1	2	2	2	2	2	3	3	4	4	4	3	4
CH_3 sym. def.	3	2	2	2	1	1	1	0	0	0	0	0	0
Total	14	16	16	16	11	12	18	14	20	20	20	15	20
600-1100 cm^{-1}													
CH_2 twist.	1	2	2	2	1	2	3	2	4	4	4	3	4
C-C stretch.	1	2	2	2	2	2	3	3	4	4	4	3	4
$(CH_3)'$ rock.	2	4	4	4	3	4	6	5	8	8	8	6	8
CH_3 rock.	6	4	4	4	1	1	2	0	0	0	0	0	0
CH_2 rock.	1	2	2	2	1	2	3	2	4	4	4	3	4
Total	11	14	14	14	8	11	17	12	20	20	20	15	20

TABLE XVIII--Continued

Region and Characteristic Vibration	Molecular Symmetry												
	TMEL	DMDEL			MTEL			TEL					
	C_s	C_{2v}	C_2	C_s	C_{3v}	C_3	C_s	D_{2d}	C_{2v}	C_2	D_2	S_4	C_s
400-600 cm^{-1}													
Pb-C stretch.	3	2	2	2	1	1	1	0	0	0	0	0	0
(Pb-C)' stretch.	1	2	2	2	2	2	3	3	4	4	4	3	4
Total	4	4	4	4	3	3	4	3	4	4	4	3	4
200-400 cm^{-1}													
$(CH_3)'$ torsion	1	2	2	2	1	2	3	2	4	4	4	3	4
CH_3 torsion	3	2	2	2	0	1	1	0	0	0	0	0	0
Pb-C-C bending	1	2	2	2	2	2	3	3	4	4	4	3	4
Total	5	6	6	6	3	5	7	5	8	8	8	6	8
100-200 cm^{-1}													
Pb-C-C twisting	1	2	2	2	1	2	3	2	4	4	4	3	4
C-Pb-C def.	5	5	5	5	3	3	5	4	5	5	5	4	5
Total	6	7	7	7	4	5	8	6	9	9	9	7	9

[a] $(CH_3)'$ = methyl group not bonded directly to lead atom; (Pb-C)' = lead-carbon bond between lead atom and methylene group.

TABLE XIX

NUMBER OF INFRARED ACTIVE FUNDAMENTALS EXPECTED IN DIFFERENT FREQUENCY REGIONS FOR DIFFERENT MOLECULAR SYMMETRIES[a]

Region and Characteristic Vibration	Molecular Symmetry												
	TMEL	DMDEL			MTEL			TEL					
	C_s	C_{2v}	C_2	C_s	C_{3v}	C_3	C_s	D_{2d}	C_{2v}	C_2	D_2	S_4	C_s
2800-3000 cm^{-1}													
$(CH_3)'$ asym. str.	2	3	4	4	3	4	6	3	6	8	6	4	8
CH_3 asym. str.	6	3	4	4	1	1	2	0	0	0	0	0	0
CH_2 asym. str.	1	1	2	2	1	2	3	1	2	4	3	2	4
$(CH_3)'$ sym. str.	1	2	2	2	2	2	3	2	4	4	3	2	4
CH_3 sym. str.	3	2	2	2	1	1	1	0	0	0	0	0	0
CH_2 sym. str.	1	2	2	2	2	2	3	2	4	4	3	2	4
Total	14	13	16	16	10	12	18	8	16	20	15	10	20
1100-1500 cm^{-1}													
$(CH_3)'$ asym. def.	2	3	4	4	3	4	6	3	6	8	6	4	8
CH_3 asym. def.	6	3	4	4	1	1	2	0	0	0	0	0	0
CH_2 def.	1	2	2	2	2	2	3	2	4	4	3	2	4
CH_2 wagging	1	2	2	2	2	2	3	2	4	4	3	2	4
$(CH_3)'$ sym. def.	1	2	2	2	2	2	3	2	4	4	3	2	4
CH_3 sym. def.	3	2	2	2	1	1	1	0	0	0	0	0	0
Total	14	14	16	16	11	12	18	9	18	20	15	10	20
600-1100 cm^{-1}													
CH_2 twist.	1	1	2	2	1	2	3	1	2	4	3	2	4
C-C stretch.	1	2	2	2	2	2	3	2	4	4	3	2	4
$(CH_3)'$ rock.	2	3	4	4	3	4	6	3	6	8	6	4	8
CH_3 rock.	6	3	4	4	1	1	2	0	0	0	0	0	0
CH_2 rock.	1	1	2	2	1	2	3	1	2	4	3	2	4
Total	11	10	14	14	8	11	17	7	14	20	15	10	20

TABLE XIX--Continued

Region and Characteristic Vibration	Molecular Symmetry												
	TMEL	DMDEL			MTEL			TEL					
	C_s	C_{2v}	C_2	C_s	C_{3v}	C_3	C_s	D_{2d}	C_{2v}	C_2	D_2	S_4	C_s
400-600 cm^{-1}													
Pb-C stretch.	3	2	2	2	1	1	1	0	0	0	0	0	0
(Pb-C)' stretch.	1	2	2	2	2	2	3	2	4	4	3	2	4
Total	4	4	4	4	3	3	4	2	4	4	3	2	4
200-400 cm^{-1}													
$(CH_3)'$ torsion	1	1	2	2	1	2	3	1	4	4	3	2	4
CH_3 torsion	3	1	2	2	0	1	1	0	0	0	0	0	0
Pb-C-C bending	1	2	2	2	2	2	3	2	4	4	3	2	4
Total	5	4	6	6	3	5	7	3	8	8	6	4	8
100-200 cm^{-1}													
Pb-C-C twisting	1	1	2	2	1	2	3	1	2	4	3	2	4
C-Pb-C def.	5	4	5	5	3	3	5	2	4	5	3	2	5
Total	6	5	7	7	4	5	8	3	6	9	6	4	9

[a] $(CH_3)'$ = methyl group not bonded directly to lead atom; (Pb-C)' = lead-carbon bond between lead atom and methylene group.

comparison, the available data for the analogous silicon series are shown in Fig. 22, page 108. The Raman data for the lead alkyls and the infrared data for MTEL, TEL, and TEL-d_{20} are taken from the present work, while the infrared spectrum shown for TML is that of Swanson (18), and for TMEL and DMDEL, are those obtained in the Ethyl Corporation Research Laboratories (6). The Raman and infrared data for tetramethylsilane are those reported by Rank (16), while the Raman data for the intermediate silicon alkyls are those of Kolesova (13), and for tetraethylsilane, are those of Anderson (1).

In the following discussion, the term "band" is used empirically and will generally include a number of coincident or overlapping bands.

The 2800 - 3000 cm^{-1} Region

Sic different "group frequencies" are expected in this region, as shown in Tables XVIII and XIX, pages 102 - 104, respectively. Good infrared data are not available because of the low dispersion here. In TMEL, DMDEL, and MTEL, six Raman bands interpreted as fundamentals are observed in this region, their frequencies and relative intensities being nearly unchanged throughout the series. In TEL only five of the six are observed, the band of highest frequency being absent.

All members of the series have a Raman band near the

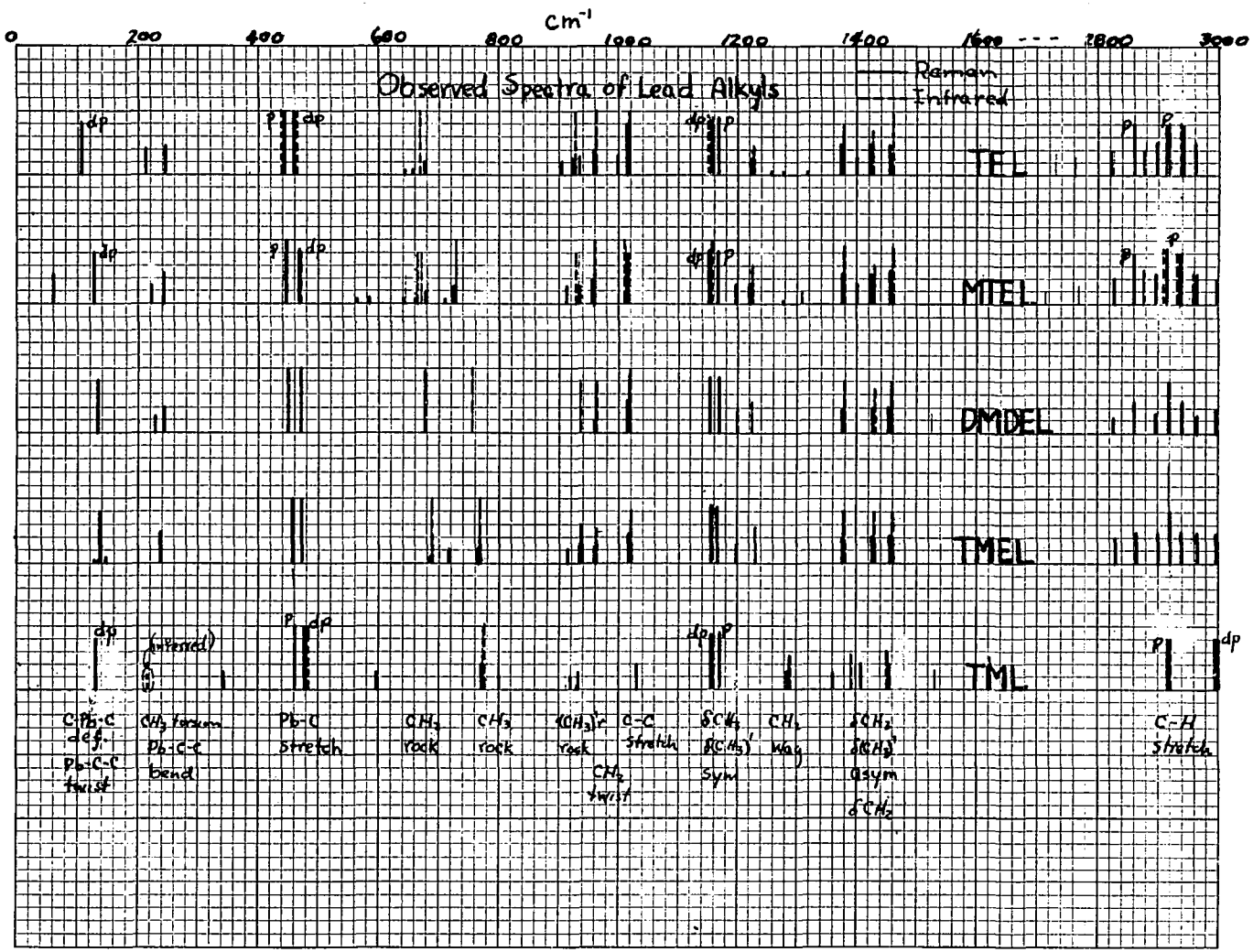

Fig. 21. Observed Spectra of Lead Alkyls

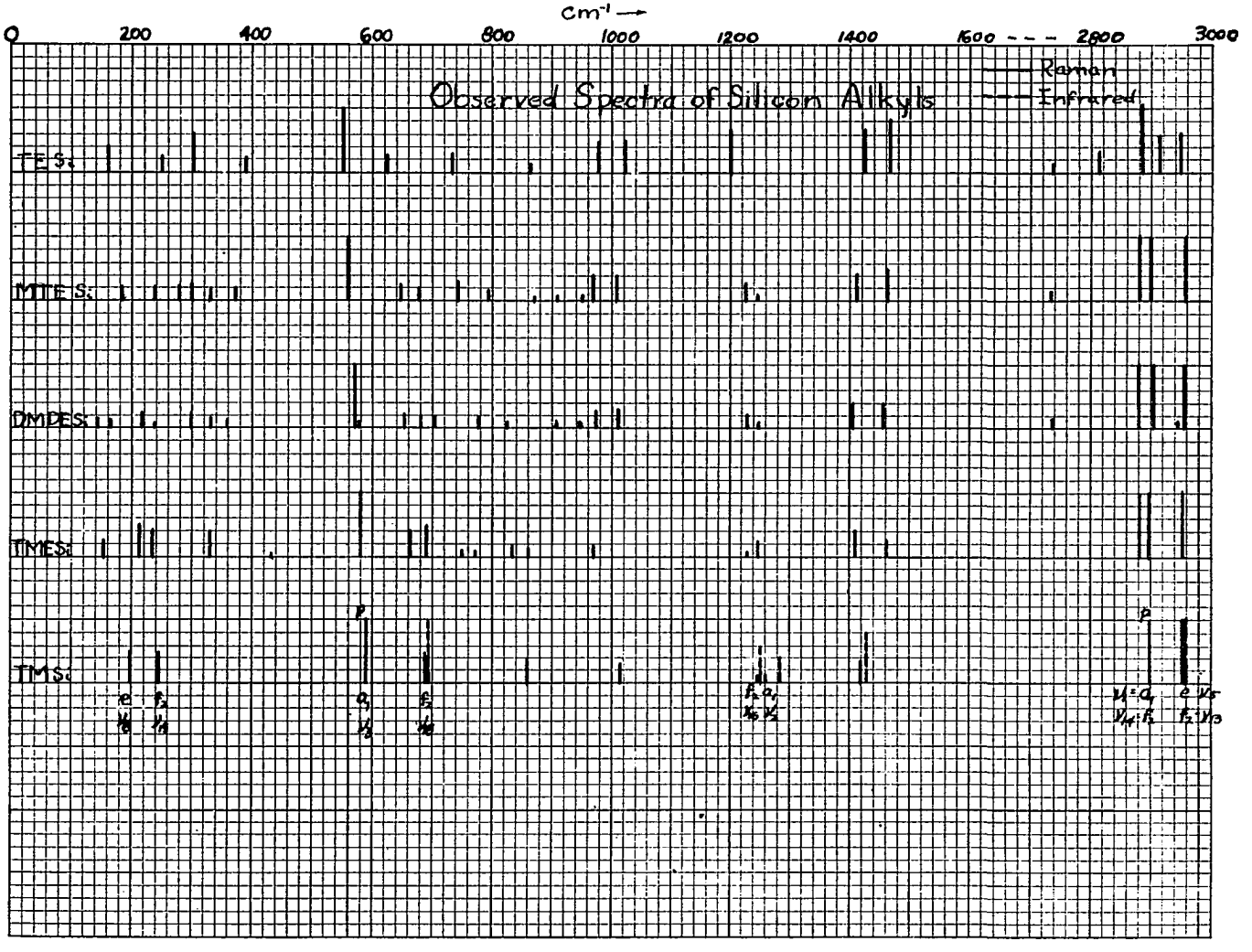

Fig. 22. Observed Spectra of Silicon Alkyls

2918 cm^{-1} Raman band in TML. However, bands near the 2998 cm^{-1} Raman band in TML are found only in TMEL, DMDEL, and MTEL. The Raman band near 2918 cm^{-1} is sharper in the other molecules than in TML, whereas the 2998 cm^{-1} band has about the same appearance. Since the Raman band at 2918 cm^{-1} in TML is interpreted as superposed a_1 and f_2 symmetrical CH_3 stretching vibrations, the corresponding band in the other spectra are probably also caused by symmetrical methyl stretching. The fact that the band appears practically unchanged in TEL, which has only methyl groups that are not bonded directly to the lead atom, shows that the C-H stretching vibration in such methyl groups, here denoted by $(CH_3)'$, has very nearly the same frequency as in CH_3 groups bonded directly to the lead atom.

The Raman band at 2998 cm^{-1}, found in TMEL, DMDEL, and MTEL, but not in TEL, is due to asymmetrical C-H stretching in the methyl groups bonded directly to lead. In the methyl groups not bonded directly to lead, this vibration appears to give rise to a Raman band near 2960 cm^{-1}. The Raman band near 2940 cm^{-1} may arise from asymmetric, and the Raman band near 2960 cm^{-1} from symmetric C-H stretching in methylene groups, since they first appear in TMEL and grow stronger as the number of methylene groups is increased. The Raman bands occurring near 2900 and 2830 cm^{-1} in all the lead alkyls except TML may be fundamental symmetric stretching modes in the CH_3 or CH_2 groups, or they may be the overtones

of 1455 and 1425 cm^{-1}, intensified and shifted somewhat by the interaction with fundamentals of the proper species and perhaps overlapped by other C-H stretching modes.

The 1100 - 1500 cm^{-1} Region

Six different "group" frequencies are listed for this region in Tables XVIII and XIX, pages 102, and 104, respectively. The CH_2 twisting vibrations may also be here, but since the effect of the lead atom would seem to be to shift these vibrations to lower frequencies, they will be discussed together with the vibrations expected in the 600 - 1100 region. In the Raman spectrum of each molecule there are five observed bands at approximately 1155, 1164, 1375, 1425, and 1456 cm^{-1}, which appear nearly unchanged in frequency and relative intensity throughout the series. Bands are also observed near 1375, 1425 and 1456 cm^{-1} in the infrared spectra of all the molecules.

The normal paraffins have a band (sometimes a doublet) at about 1460 cm^{-1} which is interpreted as due to CH_2 deformations and asymmetric CH_3 deformations. Since the asymmetric methyl deformation $\nu_{15}(f_2)$ in TML is assigned the frequency 1455 cm^{-1}, at least one member of the apparently double band observed in both Raman and infrared spectra at about 1456 cm^{-1} is probably caused by asymmetrical deformation of methyl groups, either bonded directly to the lead atom or separated from it by a CH_2 group.

The bands observed in both infrared and Raman spectra at 1375 and 1425 cm^{-1} may be ascribed to asymmetrical CH_3 deformation and CH_2 deformation, respectively, the shift of the latter from its position at 1460 cm^{-1} in the paraffins being caused by the proximity of the lead atom. These bands may also result from Fermi coupling between the asymmetrical CH_3 deformation and the combination bands 240 + 1155 = 1395 cm^{-1} or 240 + 1164 = 1405 cm^{-1}. If the band at 1425 cm^{-1} is so interpreted, the fundamental involving CH_2 deformation should be assigned to one member of the doublet near 1460 cm^{-1}. The sharpness of the Raman bands at 1375, 1425, and 1460 cm^{-1} indicates that Coriolis coupling between the different vibrations does not occur, unlike the case of TML.

The normal paraffins have a band at 1380 cm^{-1} that is interpreted as due to symmetric methyl deformation. Fig. 20, page 95, shows the lowering of this frequency in $(CH_3)_4$ X-type molecules from its value near 1380 cm^{-1} in tetramethylmethane to approximately 1160 cm^{-1} in tetramethyllead. It might be expected that for the methyl groups not bonded directly to the lead atom, in the methyl-ethyl alkyls and in TEL, these vibrations would lie near 1380 cm^{-1}. However, the most striking feature of the spectra of the lead alkyls is the constancy in frequency and intensity of the Raman bands near 1155 and 1165 cm^{-1} throughout the entire series of compounds. This indicates strongly that the symmetrical methyl deformations have practically the same frequency for the methyl

groups (CH_3) and $(CH_3)'$. From this the remarkable conclusion may be drawn that the symmetrical methyl deformations are affected by the lead atom to the same degree in methyl groups not bonded directly to the lead atom and in methyl groups so bonded.

The only infrared spectra of TMEL and DMDEL available are those obtained by the Ethyl Corporation on a Beckman IR-2 spectrometer with cells of 0.1 mm and 0.5 mm thickness. In these spectra a band is observed near 1160 cm^{-1}, but it is not possible to decide whether this represents one band or the superposition of bands near 1155 and 1165 cm^{-1}. In the present work a single infrared band is observed at 1155 cm^{-1} in both MTEL and TEL. Since the resolving power of the Perkin-Elmer Model 112 spectrometer should suffice to separate bands at 1155 and 1164 cm^{-1} if they were both infrared-active, it is concluded that the observed infrared band is not a superposition of bands at these frequencies. This agrees with the infrared data for TEL reported by Swanson (18).

Since the Raman band at 1164 cm^{-1} is polarized in both TEL and MTEL, these molecules must have a totally symmetric vibration with this frequency. This implies that TEL has the symmetry D_{2d}, since this is the only symmetry of TEL that allows a totally symmetric Raman active, but infrared inactive methyl deformation. This, however, is not in accord with the view that TEL exists in several different symmetry configurations, which seems necessary to interpret the bands

at 443 and 462 cm^{-1}.

No symmetry of MTEL allows a Raman active, but infrared inactive, fundamental. However, there are configurations with symmetry C_3 for which totally symmetric methyl deformations would have a small net dipole moment and produce very weak infrared absorption bands.

Sharp Raman bands are observed in TMEL at 1196 cm^{-1} and in MTEL and TEL at 1225 and 1318 cm^{-1}. A Raman exposure of DMDEL strong enough to show a band near these frequencies was not obtained. However, the infrared spectra of all four compounds show a band at 1225 cm^{-1}. These bands at 1196, 1225, and 1318 cm^{-1} may be due to CH_2 wagging fundamentals.

In addition to these sharp bands, a very weak, diffuse Raman band, which may be due to a combination of lower frequency fundamentals, appears superposed on the strong, sharp bands at approximately 1425 and 1460 cm^{-1} in TMEL, MTEL, and TEL.

The 600 - 1100 cm^{-1} Region

Five different "group frequencies" are expected in this region: C-C stretching, CH_3, $(CH_3)'$, and CH_2 rocking, and, perhaps, CH_2 twisting. The number of each of these for different molecular symmetries is given in Tables XVIII and XIX, pages 102, and 104, respectively.

The sharp Raman and infrared bands at approximately 1015 cm^{-1} in all the alkyls except TML is almost certainly

a C-C stretching fundamental. The band at 960 cm^{-1} may be ascribed to rocking of the methyl group not bonded directly to the lead atom, and the band at approximately 936 cm^{-1} to the overtone of the band near 472 cm^{-1}, although several combination bands seem to imply the existence of a fundamental near this frequency.

The infrared and Raman bands at 764 cm^{-1} in TMEL probably involve rocking of the methyl groups bonded directly to the lead atom, since these vibrations lie near this frequency in TML. A Raman spectrum strong enough to show the presence or absence of this band in DMDEL was not obtained. However, the infrared spectrum obtained by the Ethyl Corporation (6) seems to show a band at this frequency. The band at 728 cm^{-1} in MTEL may be either CH_2 rocking or possibly a rocking of the single methyl group bonded directly to the lead atom.

The sharp Raman band near 670 cm^{-1} and perhaps the bands at 640 and 660 cm^{-1} in both MTEL and TEL may be due to CH_2 rocking although they may also be explained as combination bands.

The 400 - 600 Region

All the lead alkyls have two strong Raman bands similar in appearance to the bands at 462 and 475 cm^{-1} in TML and at nearly these frequencies. As in TML, the band at the lower frequency is polarized and the other depolarized in both MTEL and TEL. Polarization data are not available for TMEL and

DMDEL. Infrared bands were found at approximately 445 and 465 cm^{-1} in both MTEL and TEL. The work of Pitzer and Sheline (17) shows that in TML only the vibration of higher frequency is observed in the infrared, in agreement with its assignment as an f_2 fundamental in TML and the assignment of the band of lower frequency as a totally symmetric fundamental.

For TEL these bands may be interpreted under two different assumptions. If TEL is assumed to have the symmetry D_{2d}, there must, according to Table XVI, page 85, be at least two vibrations with frequency 443 cm^{-1}, one of which must be totally symmetric, giving rise to the observed polarized Raman band, while the other must belong to either species b_2 or e to account for the infrared activity. If the band at 443 cm^{-1} is assumed to be caused by only one fundamental, it must be totally symmetric, since it is polarized. The molecule must then exist in a configuration with symmetry other than D_{2d}, to account for the infrared activity of the band. However, if TEL exists in appreciable amount with symmetry other than D_{2d}, the symmetrical methyl deformation at 1164 cm^{-1} should be observable in the infrared, contrary to experimental evidence.

The difficulty with the interpretation of the TEL band at 443 cm^{-1} does not arise for MTEL, since all of its fundamentals are both infrared and Raman active for any possible molecular symmetry.

The 200 - 400 cm^{-1} Region

The "group frequencies" expected here are associated with CH_3 torsion and Pb-C-C bending. Their numbers for each compound are given for different molecular symmetries in Tables XVIII and XIX, pages 102, and 104. On the assumption made about its symmetry, TML has no active fundamentals in this region. However, it was shown in Chapter VI that there is some indirect evidence for a torsional frequency near 215 cm^{-1}. TMEL has a single band at 235 cm^{-1}, while DMDEL, MTEL, and TEL all have Raman bands at approximately 225 cm^{-1} and 240 cm^{-1}. Detailed assignments are not possible at present.

The 0 - 200 cm^{-1} Region

The vibrations expected in this region are those involving C-Pb-C bending and Pb-C-C twisting, the latter being predicted on the assumption that the potential barrier for these vibrations is roughly the same as for the torsional oscillations of the methyl groups in TML which occur at approximately 215 cm^{-1}. The number of such vibrations is given in Table XVIII, page 102 .

The Raman spectrum of each molecule has a strong, diffuse band in this region. The band center is at approximately 132 cm^{-1} in TML, and is lowered as the number of ethyl groups is increased, appearing at about 107 cm^{-1} in TEL. In addition, TMEL has three sharp Raman bands at 127, 134, and

144 cm^{-1} superposed on this diffuse band, while MTEL seems to have a sharp band at 60 cm^{-1}. It is not possible at the present time to make a detailed assignment of the fundamentals in this region. Moreover, no explanation has been found for the possibly spurious band at 60 cm^{-1}, which can hardly be a fundamental of the MTEL molecule.

CHAPTER VIII

COMPARISON OF THE SPECTRA OF TEL AND TEL-d_{20}

The observed infrared and Raman spectra are compared in Fig. 23, page 119. No difficulty is encountered in correlating the bands* representing Pb-C stretching, C-Pb-C deformation, Pb-C-C bending and twisting, $(CH_3)'$ torsion, and CH_2 rocking. On the other hand, the correlation of individual bands involving C-H stretching is somewhat uncertain, and there is considerable doubt concerning the correlation of some of the bands arising from symmetric and asymmetric methyl deformation, C-C stretching, CH_2 deformation CH_2 wagging and twisting, and $(CH_3)'$ rocking.

The two strong Raman and infrared bands involving Pb-C stretching at 443 and 460 cm^{-1} in TEL are shifted to 401 and 416 cm^{-1} in TEL-d_{20}. In place of the two Raman bands at 243 and 213 cm^{-1} in TEL, interpreted as due to Pb-C-C bending and $(CH_3)'$ torsion, there are three bands at 217, 196, cm^{-1} in TEL-d_{20}. The diffuse band with center at approximately 107 cm^{-1} in TEL, associated with skeletal deformation

---

*In the following discussion the term "band" means observed band.

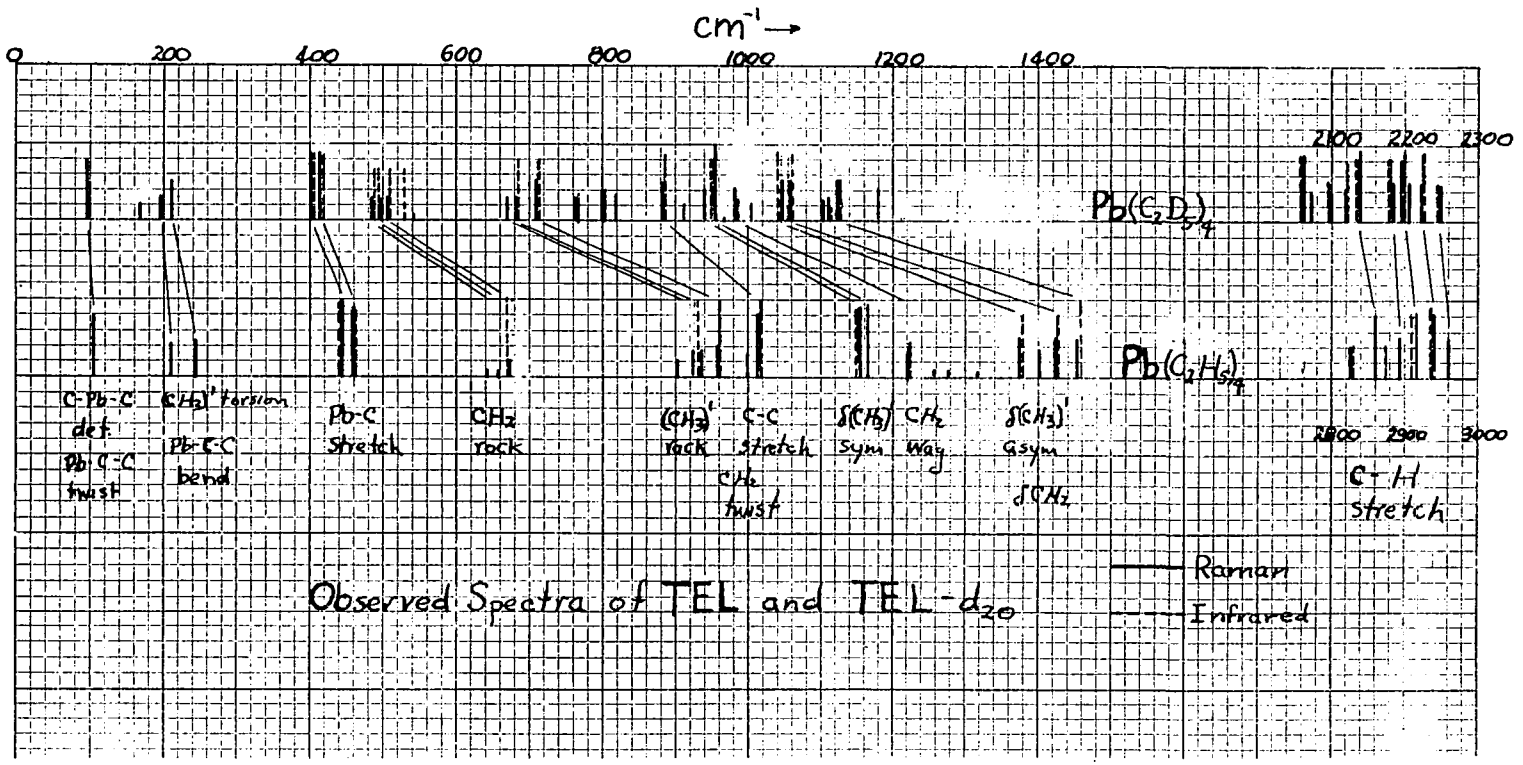

Fig. 23. Observed Spectra of TEL and TEL-d_{20}

and Pb-C-C twisting, is shifted to about 95 cm^{-1} in TEL-d_{20}. The three weak Raman bands at 674, 657, and 641 cm^{-1}, which may be ascribed to CH_2 rocking, are shifted to 509, 497, and 484 cm^{-1}, respectively. These bands were not resolved in the infrared spectrum of TEL because of the low transmission of the NaCl prism and the poor dispersion of the CsBr prism in this region.

The characteristic group of bands associated with C-H stretching in the 2800 - 3000 cm^{-1} region of the Raman spectrum of TEL have a counterpart with nearly the same pattern between 2050 and 2250 cm^{-1} in TEL-d_{20}. Slight differences, however, make a band for band correlation difficult. In this region, the infrared spectrum of TEL-d_{20} corresponds band for band to the observed Raman spectrum. However, for TEL, the low resolution near 3000 cm^{-1} makes it difficult to determine which bands are infrared active.

The Raman bands at 2960 and 2940 cm^{-1} in TEL probably correspond to the bands at 2247 and 2223 cm^{-1}, respectively, in TEL-d_{20}. The TEL bands at 2918 and 2895 cm^{-1} may correspond to the TEL-d_{20} bands at 2207 and 2197 cm^{-1}, or the latter bands may result from a splitting of the band corresponding to the band at 2918 cm^{-1} in TEL. A comparison of the relative intensities of the bands in each spectrum favors the latter interpretation. The TEL band at 2895 cm^{-1} would then correspond to the band at 2183 cm^{-1} in TEL-d_{20}, while the TEL bands at 2860 and 2824 cm^{-1} may correspond to those

at 2139 and 2061 cm^{-1}, respectively, in TEL-d_{20}.

In the Raman spectrum of TEL-d_{20}, there are two sharp bands at 1047 and 1058 cm^{-1}, while in the infrared spectrum a band at 1047 cm^{-1} appears as a shoulder on a band at 1058 cm^{-1}. These bands probably correspond to the Raman and infrared bands at 1373 and 1424 cm^{-1} in TEL. The infrared and Raman bands of TEL-d_{20} at 1124, and the two weak Raman bands at 1104 and 1113 cm^{-1}, may correspond to the apparently double band at 1458 cm^{-1} in both spectra of TEL. The TEL-d_{20} band at 982 cm^{-1} probably corresponds to the bands observed at 1225 cm^{-1} in TEL.

In place of the strong Raman band at 1164 cm^{-1} and the intense Raman and infrared bands at 1155 cm^{-1} in TEL, a very strong, sharp Raman band and a strong sharp infrared band at 955 cm^{-1} are observed in TEL-d_{20}. In addition, a weak, sharp Raman band appears at 940 cm^{-1}. The band at 955 cm^{-1}, which is the strongest band in the Raman spectrum of TEL-d_{20}, is very sharp and appears to be a single band, while the two Raman bands at 1155 and 1164 cm^{-1} in TEL are of nearly equal intensity. This makes the correlation of these bands somewhat uncertain. The infrared and Raman bands at 1014, 958, 936, and 928 cm^{-1} in TEL appear to be shifted to 883, 710, 683, and 672 cm^{-1}, respectively, in TEL-d_{20}.

All attempts to make detailed assignments of fundamentals for TEL and TEL-d_{20}, and to check these with the Teller-Redlich product rule, have been unsuccessful. This

failure has been caused by the complexity of the molecules and perhaps even more by the existence of several molecular equilibrium configurations.

CHAPTER XIX

SUMMARY AND CONCLUDING REMARKS

Techniques have been developed for handling the unstable lead alkyls and for obtaining Raman spectra at temperatures so low that photochemical decomposition is negligible. For tetraethyllead, the most unstable of these compounds, this temperature is approximately -120°C. Very strongly exposed Raman spectra were obtained for all the lead alkyls, including TEL-d_{20}, for which no previous Raman or infrared data existed. The Raman spectrum of a crystalline aggregate of TML at -70°C, and of the extremely unstable triethylbismuth in the liquid state at -125°C, were also obtained.

Infrared spectra of liquid MTEL, TEL, TEL-d_{20} were obtained in the region from 3 to 25 microns with the aid of a Perkin-Elmer Model 112 spectrometer.

The spectra obtained are discussed and compared with those reported by previous workers. There are several frequencies that appear practically unchanged throughout the entire series TML to TEL. These frequencies are: 130, 462, 475, 1155, 1165, and 2918 cm^{-1}. In addition, several differences are noted between the spectra of TML and those of the

other molecules.

An assignment of the fundamental vibrational frequencies has been made for TML, assumed to have the symmetry T_d, and compared in detail with previous assignments. One of the principal differences between these assignments and the one given here is the interchange of the assignments for the fundamentals $\nu_8(e)$ and $\nu_{19}(f_2)$, involving skeletal deformations, so that ν_8 is assigned to 145 cm^{-1} and ν_{19} to 130 cm^{-1}. This assignment of the doubly degenerate fundamental to the higher frequency and the triply degenerate fundamental to the lower frequency is not in accord with previous assignments. However, it agrees with the diagram for XY_4-type molecules given by Kohlrausch (12), if the methyl groups in TML are considered to be point masses. The present work shows that both $\nu_8(e)$ and $\nu_{19}(f_2)$ are nearly pure C-Pb-C bending motions, and that $\nu_{18}(f_2)$ is nearly pure Pb-C stretching. Another difference between the present investigation and previous studies is the assignment of a CH_3 rocking fundamental $\nu_7(e)$, previously assigned by Hall to 769 cm^{-1}, to approximately 800 cm^{-1} on the basis of the resolution of a microphotometer trace of an asymmetric Raman band into two components at 769 and 800 cm^{-1}. In addition to these changes, the inactive CH_3 torsional oscillations were assigned a frequency of approximately 215 cm^{-1} on the basis of the interpretation of the Raman band at 342 cm^{-1} as due to one or more combination bands involving these inactive fundamentals and the skeletal deformations near 130 and 145 cm^{-1}.

The inactive CH_3 stretching, deformation, and rocking fundamentals, $\nu_9(f_1)$, $\nu_{10}(f_1)$, and $\nu_{11}(f_1)$ are estimated to be near 3000, 1450, and 800 cm^{-1}, respectively, since other vibrations with these approximate characters are assigned frequencies near these values.

The Raman spectrum of crystalline TML has been interpreted on the assumption that the molecular site group is T_d, T_h, or T. This assumption seems to account adequately for the splitting, in the spectra of the crystal, of vibrations of species f_2.

The various possible configurations for the lead-carbon skeleton of each of the other lead alkyls are discussed and illustrated diagramatically, and the normal vibrations are classified according to symmetry species and approximate character of vibration. Because of the complex nature of these molecules, and their different possible symmetry configurations, it has not been possible to make a complete assignment for them. However, their spectra have been interpreted on the basis of "group" frequencies, a procedure partially justified by the great similarity of the spectra of these molecules.

An outstanding feature of the Raman spectra is that intense bands, associated with symmetrical methyl deformation and occurring in the paraffins at 1380 cm^{-1}, are found at very nearly the same frequencies, 1155 and 1165 cm^{-1}, in all the lead alkyls, with the exception of TEL-d_{20}. This leads

to the remarkable conclusion that the perturbing effect of the lead atom upon a methyl group separated from it by a methylene group is practically as strong as upon a methyl group bonded directly to it. The fact that these bands are found at nearly these same frequencies in triethylbismuth indicates that the effect of the bismuth and lead atoms are practically equal.

The observed infrared spectra of TEL near 1160 cm^{-1} does not seem to support the view that this molecule exists in configurations other than D_{2d}, a view apparently required for the interpretation of the bands at 443 and 462 cm^{-1}. Attempts to apply the Teller-Redlich product rule to TEL and TEL-d_{20} have been unsuccessful, due to the complexity of the molecules and to the probable existence of several molecular symmetry configurations.

Proposals for Future Research

The infrared and Raman spectra of completely deuterated tetramethyllead would be of great value in checking the fundamental assignments for the TML molecule by means of the Teller-Redlich product rule. Also of value in checking these assignments would be high dispersion infrared spectra and the Raman spectrum of TML in the vapor state. In particular, infrared spectra obtained on a grating spectrometer in the region 130 - 145 cm^{-1} might be helpful in deciding the assignment of $\nu_8(e)$ and $\nu_{19}(f_2)$, since only the species f_2 is

infrared active for molecules of symmetry T_d.

The infrared and Raman spectra of tetrapropyllead should be of great interest since they would indicate whether the lead atom is as effective in lowering the symmetrical methyl deformation frequency when two methylene groups separate it from a methyl group as when only one methylene group is involved.

Infrared spectra of higher resolution in the region near 1160 cm^{-1} might help resolve the difficulty in the interpretation of bands near this frequency in TEL. Better infrared spectra of TMEL and DMDEL would also be desirable, since the spectra available have bands that are not well resolved.

BIBLIOGRAPHY

1. Anderson, T. F. J. Chem. Phys. 4, 161 (1936).

2. Claassen, H. H. Ph.D. Thesis, University of Oklahoma (1949).

3. Collins, R. L. Ph.D. Thesis, University of Oklahoma (1953).

4. Corning Glass Works. "Properties of Selected Commercial Glasses." Booklet, No. B-83. (Corning Glass Works, Corning, New York).

5. Duncan, A. B. F., and Murray, J. W. J. Chem. Phys. 2, 636 (1934).

6. Ethyl Corporation Research Laboratories. Private communication to J. Rud Nielsen.

7. Hall, R. W. Ph.D. Thesis, University of Oklahoma (1952).

8. Herzberg, G. "Infrared and Raman Spectra of Polyatomic Molecules" (D. Van Nostrand Company, Inc., New York, 1945), p. 100.

9. Hornig, D. F. J. Chem. Phys. 16, 1063 (1948).

10. Hudson, R. L. Ph.D. Thesis, University of Oklahoma (1949).

11. Kettering, C. F., and Sleator, W. W. Physics 4, 39 (1933).

12. Kohlrausch, K. W. F. Hand-und Jahrbuch der Chemischen Physik (Akad, Verlagses., Leipzig, 1932--), Vol. 9: die Spektren, Part VI, Ramanspektren (1943), p. 155.

13. Kolesova, V. A., Dukarskaya, E. V., and Andreev, D. N. Isvest. Nauk. S.S.S.R., Adtel. Khim. Nauk 1953, 294-7 (Chemical Abstracts - Oct. 10, 1953 - 47, 9776d).

14. Lippincott, E. R., and Tobin, M. C. J. Am. Chem. Soc. 75,

4141 (1953).

15. Pai, N. G. Proc. Roy. Soc. (London) 149A, 29 (1935).

16. Rank, D. H., Shull, E. P., and Oakwood, T. S. J. Chem. Phys. 21, 2024 (1953).

17. Sheline, R. K., and Pitzer, K. S. J. Chem. Phys. 18, 595 (1950).

18. Swanson, R. K. M. S. Thesis, University of Oklahoma (1946).

19. Young, C. W., Koehler, J. B., and McKinney, D. S. J. Am. Chem. Soc. 69, 1410 (1947).